

Impacts of Postdam Land Use/Land Cover Changes on Modification of Extreme Precipitation in Contrasting Hydroclimate and Terrain Features

ABEL T. WOLDEMICHAEL AND FAISAL HOSSAIN

Tennessee Technological University, Cookeville, Tennessee

ROGER PIELKE SR.

University of Colorado Boulder, Boulder, Colorado

(Manuscript received 14 May 2013, in final form 18 November 2013)

ABSTRACT

Understanding the impact of postdam climate feedbacks, resulting from land use/land cover (LULC) variability, on modification of extreme precipitation (EP) remains a challenge for a twenty-first-century approach to dam design and operation. In this study, the Regional Atmospheric Modeling System (RAMS, version 6.0) was used, involving a number of predefined LULC scenarios to address the important question regarding dams and their impoundments: How sensitive are the hydroclimatology and terrain features of a region in modulating the postdam response of climate feedbacks to EP? The study region covered the Owyhee Dam/Reservoir on the Owyhee River watershed (ORW), located in eastern Oregon. A systematic perturbation of the relative humidity in the initial and boundary condition of the model was carried out to simulate EP. Among the different LULC scenarios used in the simulation over the ORW, irrigation expansion in the postdam era resulted in an increase in EP up to 6% in the 72-h precipitation total. The contribution of the reservoir on EP added 8% to the 72-h total when compared to the predam LULC conditions. To address the science question, a previously completed investigation on the Folsom Dam [American River watershed (ARW)] in California was compared with the ORW findings on the basis of contrasting differences in hydroclimatology and terrain features. The results indicate that the postdam LULC change scenarios impact EP of ORW (Owyhee Dam) much greater than the EP of the ARW (Folsom Dam) because of its semiarid climate and flat terrain. EP was less sensitive to LULC changes on the windward side of the mountainous terrain of ARW as compared to the leeward side of the flat terrain of ORW.

AU1

1. Introduction

All forms of life on Earth rely on the sustainable presence of water. However, this vital resource is unevenly distributed over the world. In most cases, this uneven distribution is restored by constructing dams along rivers. Most dams provide substantial benefits to human societies and their economies (Richter and Thomas 2007). According to Oxlade (2006), dams are barriers constructed across a river to obstruct the flow of river water. Primarily, dams and reservoirs (hereafter, “dams” will be used interchangeably with “artificial reservoirs”) are used for water supply (International Commission on

Large Dams 1999). However, applications also include irrigation for agriculture, flood control, hydropower, land navigation, and recreation.

Past civilizations have used dams for their various intended purposes. To date, large numbers of dams have been constructed at different regions in the world that vary in their hydroclimatology and land features (topography). To meet future demand for water and energy, the construction of numerous large dams has also been proposed as a key solution (Graf 1999). For instance, the Southeastern Anatolia Project [Guneydogu Anadolu Projesi (GAP)] dam and irrigation project in Turkey (Schleifer 2008); the Itaipu hydroelectric dam located on the border between Brazil and Paraguay; the Three Gorges Dam (TGD) hydropower project in China (Allin 2004); and the Grand Ethiopian Renaissance (GER) hydroelectric dam on the Blue Nile River, Ethiopia, (Hammond 2013) are some recent examples

Corresponding author address: Dr. Faisal Hossain, Department of Civil and Environmental Engineering, Tennessee Technological University, 1020 Stadium Dr., Cookeville, TN 38505-0001.
E-mail: fhossain@tntech.edu

to alleviate water and energy shortages. Although the socioeconomic benefits of dams are immense, there are undeniable safety issues posed by aging dams, especially for people living in the downstream or the “inundation zone” (FEMA 2013). Structural, hydraulic, and mechanical issues are among the major risk factors that lead to dam failure and property damage. More importantly, extreme flood events that result in overtopping and unscheduled opening of spillways pose the greatest threat when potential loss of life and property are concerned (Saxena 2004).

No two dams constructed in locations that vary in their hydroclimatology and terrain pose the same risk as far as dam safety and security are concerned. However, setting variations in climatic zone and topography aside, a common issue that applies to all dams remains the same. This concerns the anthropogenic (human induced) change observed in the form of creation of reservoirs, irrigation, and downstream urbanization in the postdam era. The majority of the factors responsible for the anthropogenic changes in the postdam era become apparent only over a long period of time after the dam is operational (Woldemichael et al. 2012). The relatively immediate response of the presence of a dam is the inundation of a previously dry landscape by the formation of reservoirs. The reservoir formed can be large or small depending on the design capacity of the dam. This involves both reservoir volume and its surface area. From a hydrometeorological point of view, a newly created reservoir can modify open water evaporation and enhance moisture supply for precipitation, hence serving as a feedback on precipitation.

A method for estimating evaporative source regions for extreme precipitation (EP) at selected locations in Europe was developed in recent studies (Gangoiti et al. 2011a,b). Through the use of a mesoscale model and kinematic 3D back-trajectory techniques, their study showed that terrestrial evaporation (including from lakes and reservoirs) can play an important role in creating extreme precipitation episodes. In another study, Kunstmann and Knoche (2011) used a regional atmospheric model to track the moisture evaporated from the Lake Volta region in Ghana and followed its path until the moisture returned to the source as precipitation. Their result indicated that up to 8% of precipitation can be traced to water evaporated from the lake region. Eltahir (1989) studied the possible feedback mechanism for the annual rainfall in the Bahr el Ghazal basin in Sudan. The study concluded that it is highly likely that the open water evaporation from the Bahr River has significant effect on the climate of the nearby dry regions. Evaporative feedbacks on precipitation have also been documented in the works of Eltahir and Bras (1996).

Apart from the local evaporative feedback mechanisms established by reservoirs, dams may also influence the nearby landscape via major changes in the land use/land cover (LULC) types. For instance, if the dam is used for irrigation or for expansion of existing irrigation systems, the majority of the nearby land is generally converted to agricultural use, which will be supplied by water from the reservoir. Moreover, the land will be frequently inundated throughout the year, when the crop demand for water is met by the supply from the dams/reservoirs. Irrigation also enhances the atmospheric water vapor content through evaporation and transpiration. It also has an effect of cooling the ambient surface and near-surface temperature by decreasing the sensible heat fluxes and increasing latent heat fluxes (Boucher et al. 2004; Eungul et al. 2011), although the flux of moist enthalpy could be increased, thus increasing the convective available potential energy (CAPE; Pielke 2001).

The added moist enthalpy from irrigation tends to create strong spatial gradients of CAPE with respect to the surrounding nonirrigated landscape, which in turn can produce mesoscale wind circulations and thus enhance the likelihood for the formation of convective precipitation. When this potential for cumulus clouds is realized, precipitation enhancement due to irrigation has been observed downwind of the irrigated landscapes where temperature and CAPE are enhanced (DeAngelis et al. 2010). Surface wetness by itself may also have a strong influence on precipitation by affecting these mesoscale circulations. Previous numerical modeling studies have also suggested an enhancement of precipitation by irrigation (Sacks et al. 2008; Segal et al. 1998; Pielke and Avissar 1990; Gero et al. 2006).

Urbanization is also among the human-induced changes brought about by the advent of dams. The very reason that the downstream region of a dam may become inhabitable, owing to a reduced risk of flooding, transforms a predam landscape into an urban landscape. Urban landscapes have a tendency to modify precipitation budget and distribution, especially on the downwind direction of the cities as a result of an alteration in the surface properties (Shepherd 2005; Jin et al. 2007). Trusilova et al. (2008) investigated the effects of urbanization on European climate by using an atmospheric modeling approach for nonurban and urban scenarios. They found that urban areas produce an increase in precipitation during the winter and a decrease in the summer. One other important phenomenon that is created by urbanization is the urban heat island (UHI). UHIs induce a kind of air circulation that is characterized by differential heating capacity between the rural and urban areas (Shepherd et al. 2005). This precipitation-conductive UHI effect can also be exacerbated by the emission of pollutants from

industries, automobiles, and building facilities that can serve as cloud condensation nuclei (CCN) and ice nuclei (IN) associated with the formation of precipitation (Marshall et al. 2004; Huff 1986; Rosenfeld et al. 1995).

An important issue that must be considered for all dams is the standard (conventional) approach adopted in the estimation of probable maximum precipitation (PMP). Although moisture maximization and transposition has been the widely accepted technique for PMP estimation, there are several limitations and uncertainties that warrant the need for more accurate

AU3 methodologies (Chen and Bradley 2006; Ohara et al. 2011; Tan 2010). First, this approach only estimates a precipitation value that is larger than what has occurred historically. This fact triggers the need for revision of the PMP value each time a heavy storm occurs. Second,

AU4 the WMO (1986, p. XXX) definition of PMP is “the greatest depth of precipitation for a given duration meteorologically possible for a given size storm area at a particular location at a particular time of year, with *no allowance made for the long term climate trends.*” The lack of consideration of long-term climate trends in modifying the already estimated PMP value represents a limitation of the stationarity assumption (Hossain et al. 2012). Moreover, values of PMP that are used for dam design are derived from hydrometeorological reports (HMRs), which are arguably outdated and lack provisions for newer and better-estimated storm events (Tomlinson and Kappel 2009; Rial et al. 2004).

The direct physical impacts that reservoirs and LULC change (e.g., irrigation and urbanization) individually have on the regional climate are beginning to be understood by the scientific community. However, there are two essential aspects that require further investigation. First, their combined effect, which is apparent wherever dams are present, is still not a very well explored subject matter. Second, the characteristics of these effects for dams located in different climate zones (e.g., humid versus semiarid and arid) and topography (e.g., mountainous versus flat) are not as well understood. Hossain et al. (2012) emphasized that both observational and numerical modeling studies around the world’s large dams is key to understanding their effect on local and regional climate. Such understanding can lead to better design and operation procedures of future and aging dams, respectively.

Degu and Hossain (2012) and DeAngelis et al. (2010) quantitatively investigated, from precipitation observations, if dams are responsible for altering the frequency of downwind precipitation in the postdam era. In another study, Jeton et al. (1996) evaluated the sensitivity of streamflow to climate for two contrasting basins (i.e.,

the American River basin west of the Sierra Nevada and the Carson River basin east of the Sierra Nevada) that represent contrasting climate and topographic variability. Their study indicated that there is a difference in the mean precipitation in the two basins, although this difference did not necessarily result in a higher change in streamflow. The basic question, however, remains how climate and terrain influence precipitation. This understanding can be used for future dam design and operational planning. In recent years, the numerical modeling approach has been found to be a useful tool in this regard.

Numerical modeling approaches have been implemented in a wide range of scenarios to investigate effects of LULC changes in different hydroclimatic zones and topography. The effects of land use heterogeneities on local climate and irrigation effects on the spatial and temporal variability of vapor and energy fluxes have been modeled using atmospheric models (e.g., Stohlgren et al. 1998; Narisma and Pitman 2006; Schneider et al. 2004; Pielke et al. 1999; Marshall et al. 2004; Douglas et al. 2006). Remote sensing techniques using satellite imageries such as the Advanced Very High Resolution Radiometer (AVHRR), Moderate Resolution Imaging Spectroradiometer (MODIS), and Advanced Spaceborne Thermal Emission and Reflection Radiometer (ASTER) have also been used to analyze LULC-induced variability in energy fluxes (Carlson and Sanchez-Azofeifa 1999; Ray et al. 2003). In addition, numerical **AU5** models have been used as a means to estimate PMP through various degrees of perturbations ingested in the atmospheric fields (i.e., relative humidity, temperature, and wind speed/direction) to replicate the traditional PMP estimation procedures (Woldemichael et al. 2012; Ohara et al. 2011; Tan 2010; Abbs 1999).

In this study, we used the Regional Atmospheric Modeling System (RAMS, version 6.0), involving a number of predefined LULC scenarios, to address the important question regarding dams and their impoundments: How sensitive are the hydroclimatology and terrain features of a region in modulating the postdam response of climate feedbacks to EP? Findings of this study allowed a comparison with the findings reported in Woldemichael et al. (2012) for a contrasting hydroclimate and topography. The study first investigated the individual effects of the anthropogenic changes on extreme precipitation for the selected study site. The impact of commonly experienced LULC changes was ranked in order of the most detectable alteration of extreme precipitation. The paper is organized as follows: section 2 presents the study region. Section 3 explains the data and methodology used in the study. Section 4 discusses the various findings. Finally, section 5

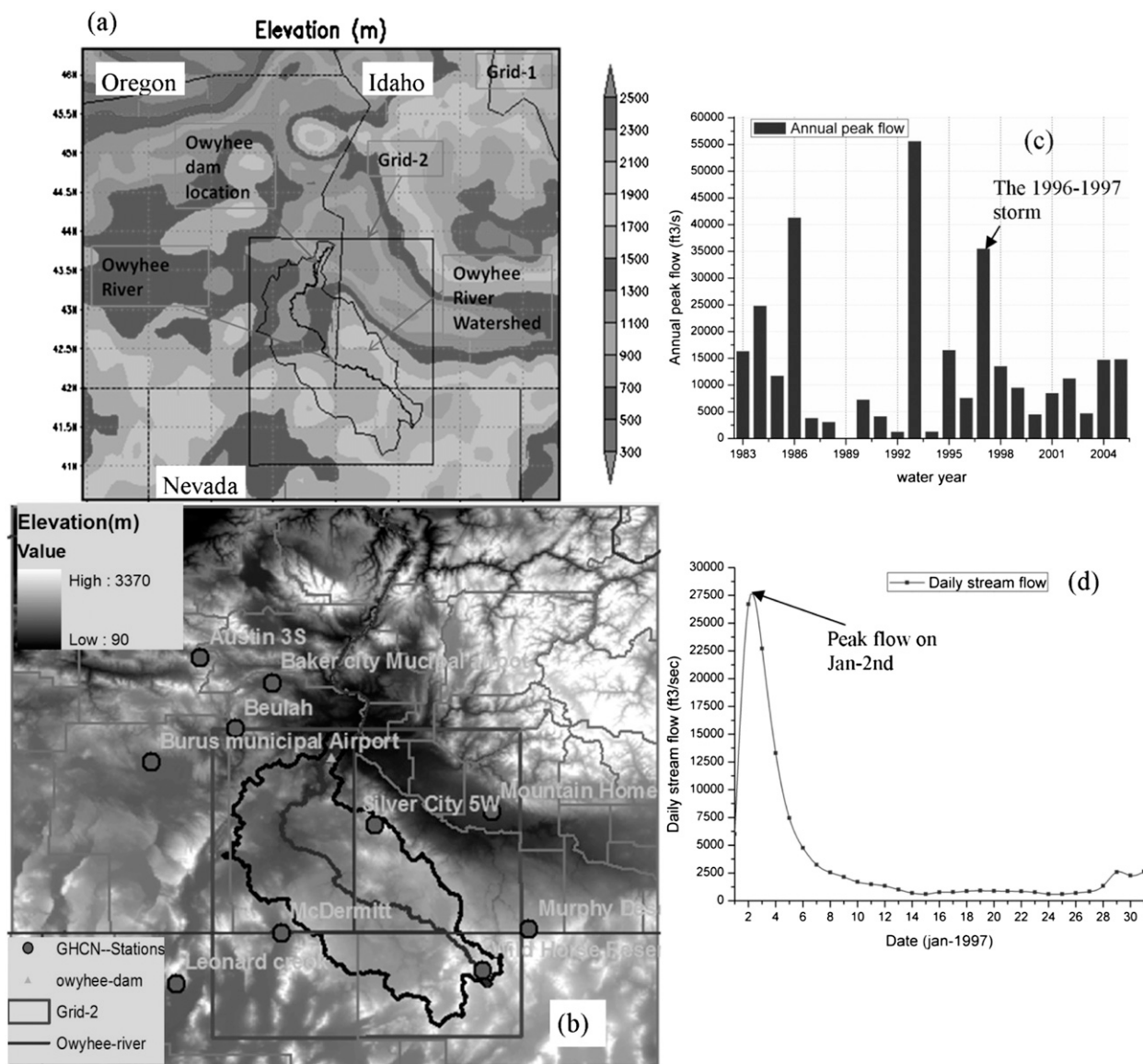


FIG. 1. (a) Topography of the ORW with grid 1 and grid 2, (b) GHCN stations on the simulation domain and Thiessen polygon around them, (c) annual peak flow ($1 \text{ ft}^3 \text{ s}^{-1} \approx 2.83 \times 10^{-2} \text{ m}^3 \text{ s}^{-1}$) near Owyhee Dam, and (d) daily streamflow on a station near Owyhee River. Panels (c) and (d) courtesy of U.S. Geological Survey (<http://waterdata.usgs.gov>).

delivers the conclusions and recommendations of the work.

2. Study region

The Owyhee Dam and Reservoir on Owyhee River, located in Malheur County, Oregon, was selected for this study (Fig. 1a). It is a concrete dam that became functional in 1932, with a reservoir capacity of 1 183 300 acre feet ($1.46 \times 10^9 \text{ m}^3$). At the time of its construction, Owyhee ranked as the world's highest dam (U.S. Bureau of Reclamation 2009). The Owyhee River watershed

(ORW) covering an area of $11\,049 \text{ mi}^2$ ($28\,617 \text{ km}^2$) made it one of the largest subbasins of the Columbia basin. Primarily, the dam has been used to irrigate the arid desert area of approximately 120 000 acres (490 km^2) over the Owyhee irrigation district. It is also used for flood damage reduction, fishery, recreation, and hydropower.

During the postdam period, there have been reported extreme flood events in the ORW. The two largest episodes occurred on 18 March 1993 and 2 January 1997 (Figs. 1c,d). During these periods, very heavy precipitation generated a runoff that forced the Owyhee reservoir

TABLE 1. Summary of model configuration used in this study.

Initialization method	Horizontally heterogeneous using NCEP–NCAR reanalysis datasets
Lateral boundary conditions	Klemp and Wilhelmson condition in which the normal velocity component specified at the lateral boundary is effectively advected from the interior assuming a propagation speed
Cumulus parameterization	Kain–Fritsch (after calibration) for grid 1, not activated for grid 2
Radiative transfer	Harrington scheme (after calibration)
Microphysics	Level-3 bulk microphysics parameterization that includes the precipitation process
Land surface model	LEAF-3 model that represents surface features interaction with the atmosphere
Diffusion scheme	Horizontal diffusion coefficients computed as the product of horizontal deformation rate and a length scale squared based on Smagorinsky formulation. Vertical diffusion is parameterized according to the Mellor and Yamada scheme, which uses a prognostic turbulent kinetic energy.

to rise to a critical level and result in an unscheduled release of water downstream. The outflow resulted in flooding as the river entered Treasure Valley near Adrian, Oregon (<http://sbk-family.us/owyhee.htm>).

In the Pacific Northwest, where the Owyhee Dam/Reservoir is located, high runoff can occur as a result of midwinter rain-on-snow effects that originate from mountains located in southwestern Idaho (such as the Owyhee Mountains; Marks et al. 2001). The flooding episode of January 1997 was driven by one such hydro-meteorological phenomenon. Apart from that, the winter of 1996/97 encountered an atmospheric river (AR) phenomenon, which transported large amounts of atmospheric moisture from the Pacific Ocean onto land (Dettinger et al. 2012). In this study, we hypothesize that the human-induced LULC change during the postdam era may have influenced the storm through land–atmosphere and reservoir–atmosphere feedback mechanisms. Thus, this study selected the 1996/97 heavy precipitation episode. The 1996/97 flood episode is also consistent with the flood period studied in a previous work on the American River watershed (ARW; Woldemichael et al. 2012), which therefore allowed a comparison of the two impounded watersheds and the role of contrasting hydro-climatology and terrain (i.e., the key science question).

3. Data and methodology

RAMS (version 6.0) was used for this study. RAMS was developed to investigate cloud and land surface atmospheric phenomena and interactions, among other atmospheric weather features (Pielke et al. 1992; Tremback et al. 1985). The model is three-dimensional and nonhydrostatic, with the horizontal grid using a rotated polar-stereographic projection to minimize distortion while the vertical structure uses a terrain-following coordinate system (Tripoli and Cotton 1980; Liston and Pielke 2000). The model’s grid-nesting capability has enabled it to include nonlinear-scale interactions and to downscale larger-scale circulations to mesoscale or

regional scales. Spatial and temporal precipitation patterns at the regional level have been adequately simulated by RAMS in previous works (e.g., Abbs 1999; Cotton et al. 2003; Nicolini et al. 2002; Woldemichael et al. 2012). RAMS also model detailed land use descriptions and various land use scenarios (Pasqui et al. 2000; Woldemichael et al. 2012).

In this study, a nested grid configuration was adopted. The grid domains are shown in Fig. 1a. The coarser grid (grid 1) consisted of 66×66 grid points at 10-km grid intervals and covered portions of Oregon, Idaho, and Nevada in between the Cascade Range in the west and the Owyhee Mountains in the east. The nested grid (grid 2) contained 86×86 grid points at 3-km grid intervals. Thirty vertical levels were assigned for both grids, with a vertical grid spacing of 100 m at the ground. The grid stretch ratio used was 1.15–1.5 km and kept constant from there on up to the model top. A 20-s time step was set for the coarser grid and 5 s for the finer grid. Table 1 provides the specific model configuration used in the study.

The Land Ecosystem–Atmosphere Feedback (LEAF) model is a submodel in RAMS that represents surface features such as soil, snow cover, vegetation, and lakes and/or oceans. It is used to evaluate the interactions between LULC and the atmosphere (Walko and Tremback 2005). A recent version, LEAF-3, was used in this study comprising 11 soil layers, one snow layer, and 10 patches per grid cell for vegetation. The soil temperature was initialized based on a default value applied horizontally homogeneously to all soil model grid points with the deep layer temperature set to be 5°C warmer than the surface. The initial soil moisture was also set to 0.35 (35% of saturation), kept constant horizontally homogeneously. The level-3 cloud microphysics parameterization was adopted for this study. This scheme predicts mixing ratio and number of concentration of rain, pristine ice crystals, snow, aggregates, graupel, and hail (Meyers et al. 1997). The Klemp and Wilhelmson lateral boundary condition scheme (Klemp and Wilhelmson 1978) was used.

The two-stream radiative parameterization was furnished by the Harrington scheme (Harrington 1997). This radiative scheme is made up of an approximate set of equations for the shortwave and longwave radiative fluxes. The equations include the influence of radiative cooling or heating from water and ice crystals in clouds. For grid 1, the Kain–Fritsch (Kain and Fritsch 1993) convective parameterization was used for deep cumulus clouds. It is a mass flux scheme that utilizes the Lagrangian parcel method, including vertical momentum dynamics, which includes the assessment of CAPE and the properties of the convective clouds, if they develop. However, this convective parameterization was switched off for grid 2, as this grid size can resolve convective activities without the use of cumulus parameterization.

The three-dimensional atmospheric variables that serve as an input for RAMS model initialization were furnished by the National Centers for Environmental Prediction–National Center for Atmospheric Research (NCEP–NCAR) reanalysis data (Kalnay et al. 1996). The surface characteristic datasets were obtained from the Atmospheric, Meteorological, and Environmental Technologies (ATMET) data archive (available at www.atmet.com). These datasets include digital elevation model (DEM) data at 30' (~1 km) spatial increments, soil moisture at various levels, the normalized difference vegetation index (NDVI), sea surface temperature (SST), and LULC. Spatial comparison of simulated precipitation values in the calibration phase was made by the help of the Parameter-Elevation Regressions on Independent Slopes Model (PRISM; available at <http://prism.oregonstate.edu>). PRISM uses point data, a DEM, and other sets of spatial datasets to generate gridded monthly and annual precipitation, among other parameters, on a 4-km spatial grid (Daly et al. 1994). Daily precipitation records were obtained from the Global Historical Climatology Network (GHCN; www.ncdc.noaa.gov).

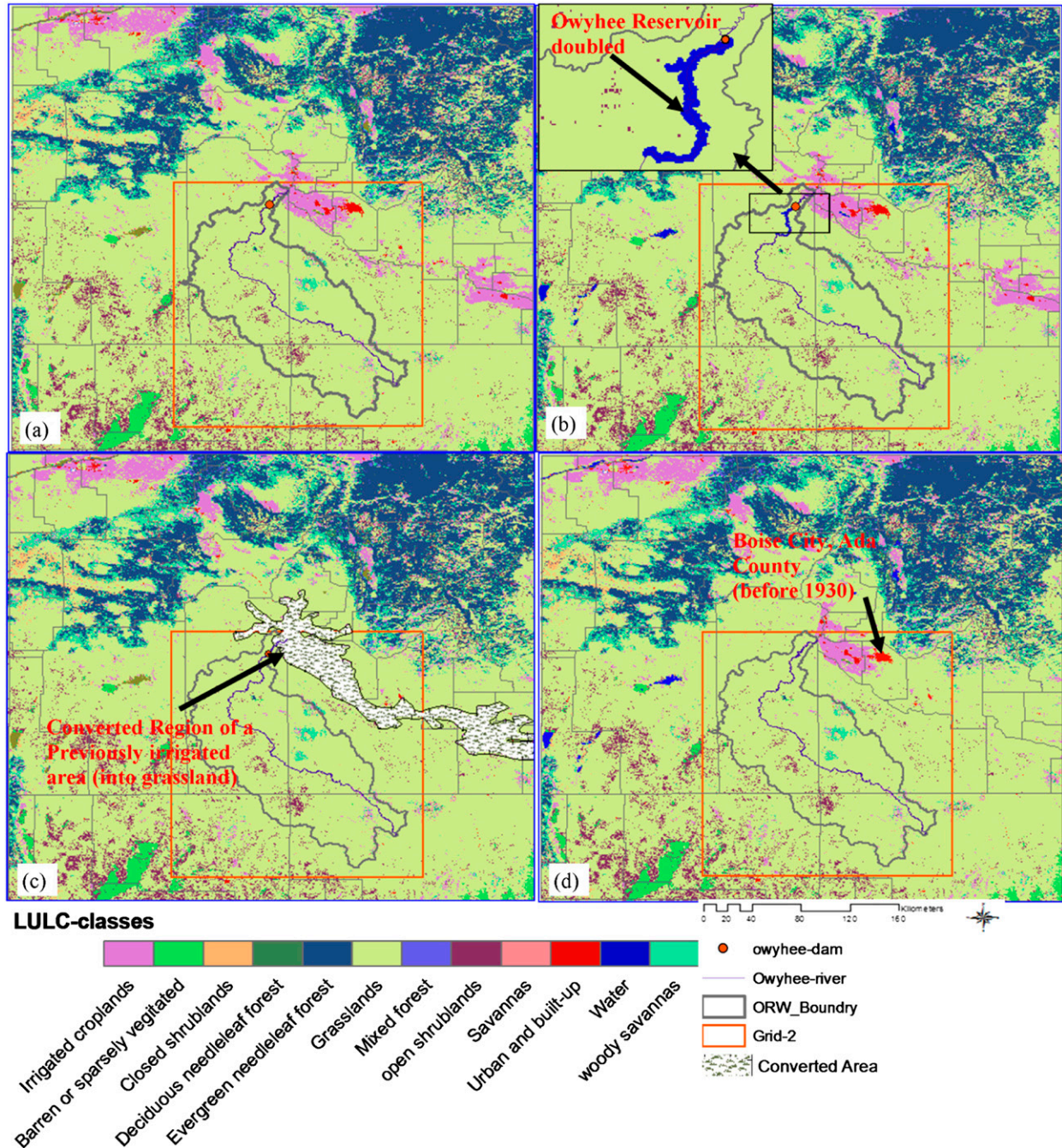
As part of the study objective, a number of LULC scenarios were created for the study of precipitation variability. There were two major sources of datasets utilized to reconstruct reservoir size as well as various LULC scenarios. The first is the History Database of the Global Environment (HYDE; <http://themasites.pbl.nl/en/themasites/hyde/index.html>) that provided gridded land use data covering over 12 000 yr (Klein Goldewijk et al. 2011). Although the HYDE dataset contained uncertainties, it is the only dataset available, to the best of our knowledge, in reconstructing the LULC conditions prior to the construction of the Owyhee Dam (before the 1930s). The second data source was the MODIS Land Cover Type 2 products from the University of Maryland (MCD12Q1; <http://glovis.gis.umd.edu/>).

Figure 2 (Fig. 2c from the HYDE dataset and the rest of the figures from MODIS) shows the reclassified LULC for use in the RAMS model obtained from the above two data sources, and Table 2 provides the percent area coverage of each LULC class for all the considered scenarios.

Major categories for the established scenarios represent the postdam and predam conditions. The postdam represents the LULC conditions long after the construction of the Owyhee Dam. Since the majority of human-induced changes are anticipated to occur in the postdam era, this category is further subdivided into the “control” (representing the existing LULC as per MODIS Land Cover Type 2 products; Fig. 2a), “reservoir double” (same as the control except the reservoir surface area is double the original capacity; Fig. 2b), and “nonirrigation” (representing the condition where previously irrigated landscape in the control over the coarser domain is transformed to the nearby land use type; Fig. 2c). The predam, with reconstructed 1930 land use, represents the landscape unaffected by human interference (Fig. 2d).

Three groups of scenarios were established to evaluate the weather feedbacks brought about by the LULC changes in the vicinity of the dam. The first scenario, the predam/postdam scenario, targeted the influence on precipitation distribution as a dam became operational. The postdam scenario, in particular, focused on quantifying the cumulative effects of downstream urbanization, flow regime change, irrigation expansion, and reservoir creation in comparison to the predam conditions. The second scenario, the reservoir–atmosphere feedback scenario, evaluated the changes in precipitation when the reservoir size changed. Finally, the land–atmosphere feedback scenario investigated the effect of presence of irrigation on extreme precipitation modification.

Two distinct types of simulations were carried out. First, a 1-month simulation (December 1996) was performed on the coarser grid (grid 1) without inclusion of the finer grid (grid 2) for the purpose of calibrating the RAMS simulations for the selected parameterization configurations. Second, an hourly simulation involving the nested grid for both the “normal” and “moisture-maximized” cases was carried out for all selected LULC scenarios. The distinction between the normal and moisture-maximized cases of simulation is that, in the former case, the atmospheric variables were unperturbed and retained their observed values. The moisture-maximized case comprised a condition where the relative humidity was systematically increased to 100% to represent full saturation in the troposphere. The standard moisture maximization procedure usually involves the



AU23 FIG. 2. The OGE reclassified LULC classes for the four scenarios: (a) control, (b) reservoir double, (c) nonirrigation, and (d) predam cases.

use of surface dewpoint temperature as an index to determine atmospheric moisture. Accordingly, two dewpoint-related values of atmospheric moisture, that is, the dewpoint representative of moisture inflow during the storm and the maximum dewpoint for the location and time considered, are determined. The respective precipitable water at these dewpoint values is then determined,

and their ratio is established as a moisture adjustment and is linearly applied to the existing amount of precipitation. However, in our study, while estimating the maximum moisture, convergence is the ideal approach to estimate the maximum possible precipitation; we chose to saturate the atmosphere with the assumption that the lateral flux of saturated air into the model domain is a reasonable

TABLE 2. Percentage coverage of the LULC classes in each of the considered scenarios.

LULC class name	Percent area (%)			
	Predam	Control	Reservoir double	Nonirrigation
Urban and built up	0.5	0.8	0.8	0.4
Evergreen needleleaf forest	32.7	32.7	32.7	32.7
Deciduous needleleaf forest	1.7	1.7	1.7	1.7
Closed shrubs	2.7	2.7	2.7	2.7
Water	0.5	0.6	0.7	0.5
Mixed forest	0.6	0.6	0.6	0.6
Irrigated croplands	13.2	14.7	14.7	10.0
Grasslands	15.9	15.7	15.7	20.0
Savannas	1.0	1.0	1.0	1.0
Barren or sparsely vegetated	2.8	2.8	2.8	2.8
Woody savanna	16.1	16.1	16.1	16.1
Open shrublands	10.5	10.6	10.6	10.5
Crops, grass, and shrubs	0.5	0.8	0.8	0.4

estimate for the maximum possible precipitation that could occur. In this study, rather than referring it as PMP, we find it more appropriate to assign the name extreme precipitation so as not to confuse this approach with the conventional engineering practice of PMP estimation from predam observations.

4. Results and discussion

a. RAMS calibration and ensemble experiments

As mentioned in section 3, a run was initiated for the whole month of December 1996 to compare the RAMS simulation with the PRISM gridded precipitation values. A combination of cumulus parameterization and radiative transfer schemes (run options) were evaluated to identify the combination that best matched with the PRISM values. The considered run options are shown in Table 3. We had to limit the selection of the parameterization into only two schemes in order to compromise with the limited resources we had to carry out more robust simulations with all the other parameterization schemes considered. Table 4 shows the monthly basin-averaged precipitation simulated by the four RAMS model run options along with the PRISM. The table also shows the difference in percent between the PRISM data and each model run options. In general, run option 4

(Kain–Fritsch and Harrington schemes) yielded relatively the most accurate result in calibration for RAMS. Figure 3 shows the spatial comparison of the PRISM versus three of the run options considered. The figure shows that the model was reasonably robust at capturing the overall spatial patterns of precipitation during the simulation period.

Further independent validation was performed with the GHCN in situ gauges located in and around the ORW (Fig. 1b). This allowed the assessment of temporal accuracy of the model simulations. The daily precipitation values simulated with RAMS were compared against the GHCN station values (Figs. 4, 5). At the point scale, the model was able to capture the precipitation trends consistently at various locations within the simulation domain.

To test the model’s signal-to-noise ratio, a perturbation ensemble experiment (not shown here) was performed through a sensitivity experiment of the initial boundary conditions. In this case, a 5% change (both increase and decrease) was introduced in the wind speed/direction, temperature, and relative humidity terms at the start of the simulation. The objective was to find out if the artificially introduced model noise of the RAMS-simulated precipitation was larger than that obtained (i.e., the signal) from the difference between

TABLE 3. The four run options explored in RAMS for model calibration.

Run option	Cumulus parameterization	Radiative transfer
1	Kuo	Mahrer and Pielke
2	Kuo	Harrington
3	Kain–Fritsch	Mahrer and Pielke
4	Kain–Fritsch	Harrington

TABLE 4. Monthly precipitation and percent difference over ORW during December 1996 by PRISM and RAMS simulations.

	PRISM	Run option 1	Run option 2	Run option 3	Run option 4
Precipitation (mm)	142	177	173	166	158
Difference (%)	—	24.65	21.83	16.9	11.27

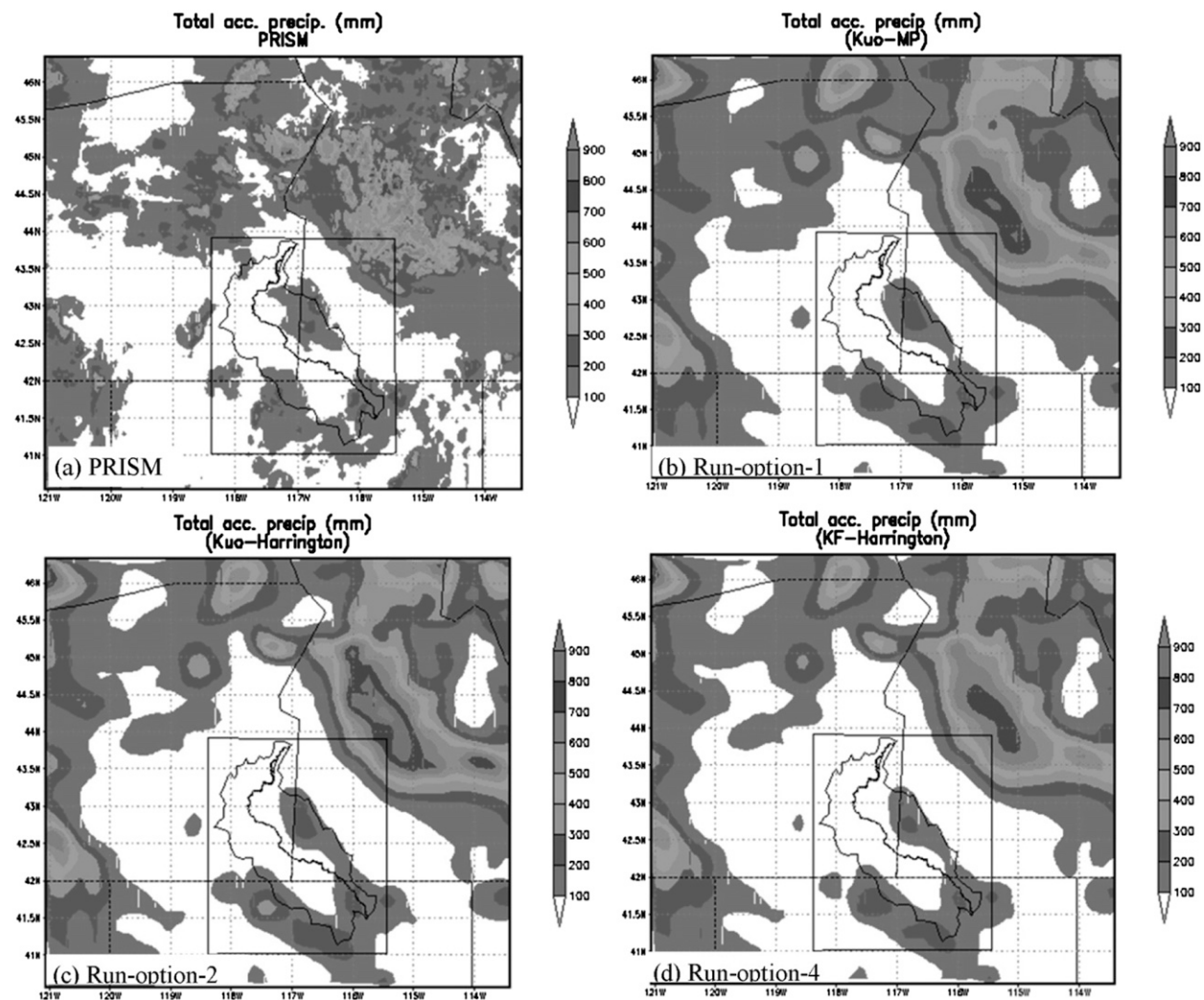


Fig. 3. Spatial comparison of monthly accumulated (Dec 1996) precipitation among (a) PRISM and (b)–(d) the other three considered run options indicated. KF is Kain–Fritsch and MP is Mahrer and Pielke.

each LULC scenarios. It was found that these ensemble experiments influenced precipitation values an order less than those shown in Figs. 4 and 5.

b. Evaluation of RAMS simulations for LULC feedback scenarios

The selected precipitation totals for analysis comprised the 24- and 72-h cumulative, which is a standard engineering practice adopted in selecting PMP values for dam design (USACE 2005). There have been number of peak flow years observed in ORW after the Owyhee Dam construction (Fig. 1c; after USGS, <http://waterdata.usgs.gov/>). The 1986 annual peak flow of more than $1133 \text{ m}^3 \text{ s}^{-1}$, the 1993 annual peak flow of approximately $1557 \text{ m}^3 \text{ s}^{-1}$, and the 1996 peak flow that generated $991 \text{ m}^3 \text{ s}^{-1}$ are among the major ones that generated more than average floods at the Owyhee Dam

outlet. Records of standard PMPs over the ORW were also published in Hydrometeorological Report (HMR) 57, which covers the Pacific Northwest states (Hansen et al. 1994). Accordingly, HMR-57 estimated the 24-h PMP value as 3.7 in. ($\sim 94 \text{ mm}$) and the 72-h PMP value as 6.15 in. ($\sim 156 \text{ mm}$).

In this study, all simulations began at 0000 UTC 21 December 1996 and ended at 0000 UTC 10 January 1997. The atmospheric fields were updated each time the NCEP–NCAR reanalysis data were available (i.e., at 6-h interval). To nudge the simulated values to the observed ones and remove any undesirable model drift, four-dimensional data assimilation (4DDA) was activated in the model. Figure 6 shows the accumulated precipitation amount for the control case (on grids 1 and 2) as well as the 24- and 72-h moving sums for normal and moisture-maximized cases of simulation, respectively. It should

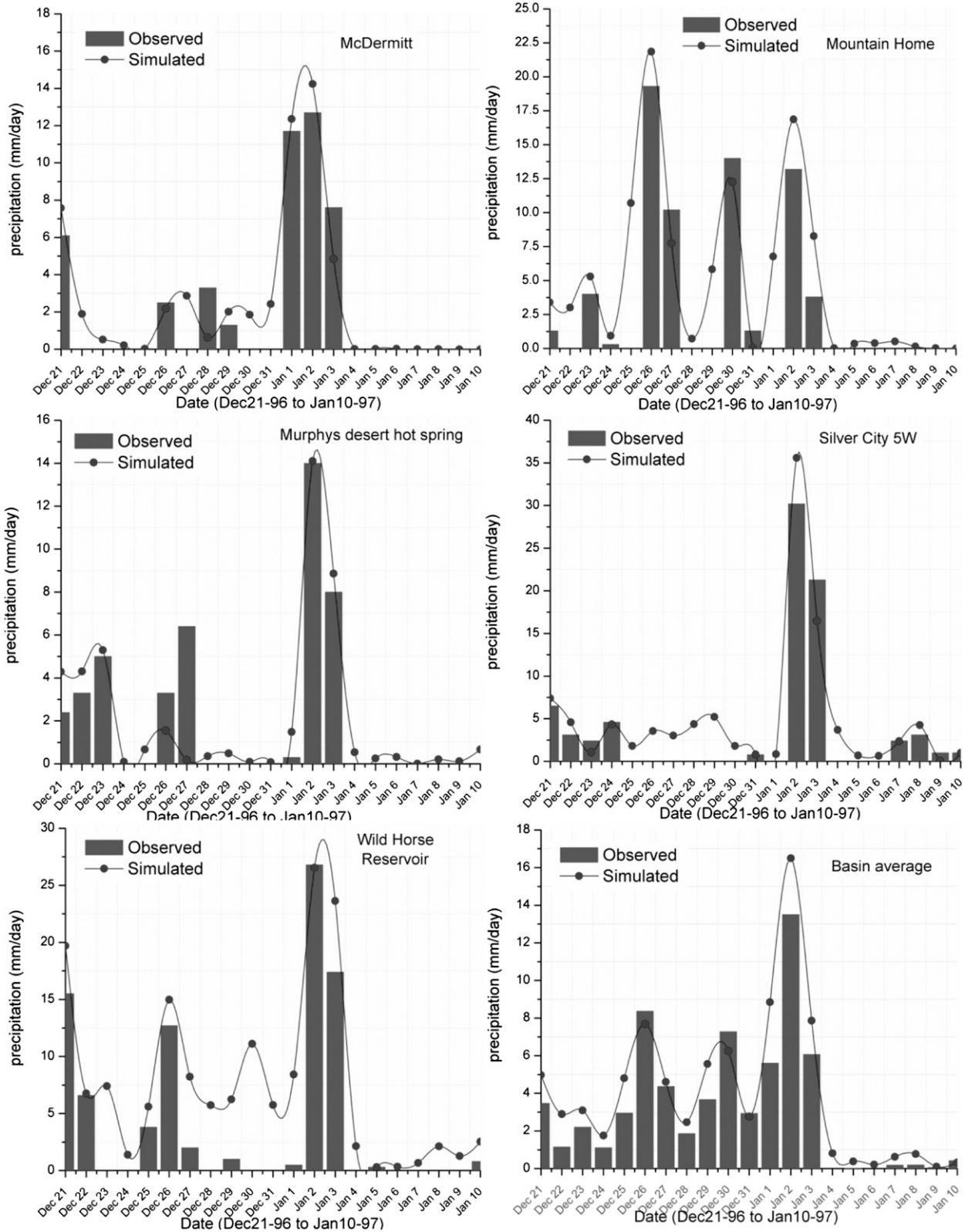


FIG. 4. Comparison of observed and simulated daily precipitation (mm day^{-1}) at selected GHCN stations within grid 2 of ORW extent during the 1996/97 storm event.

AU24

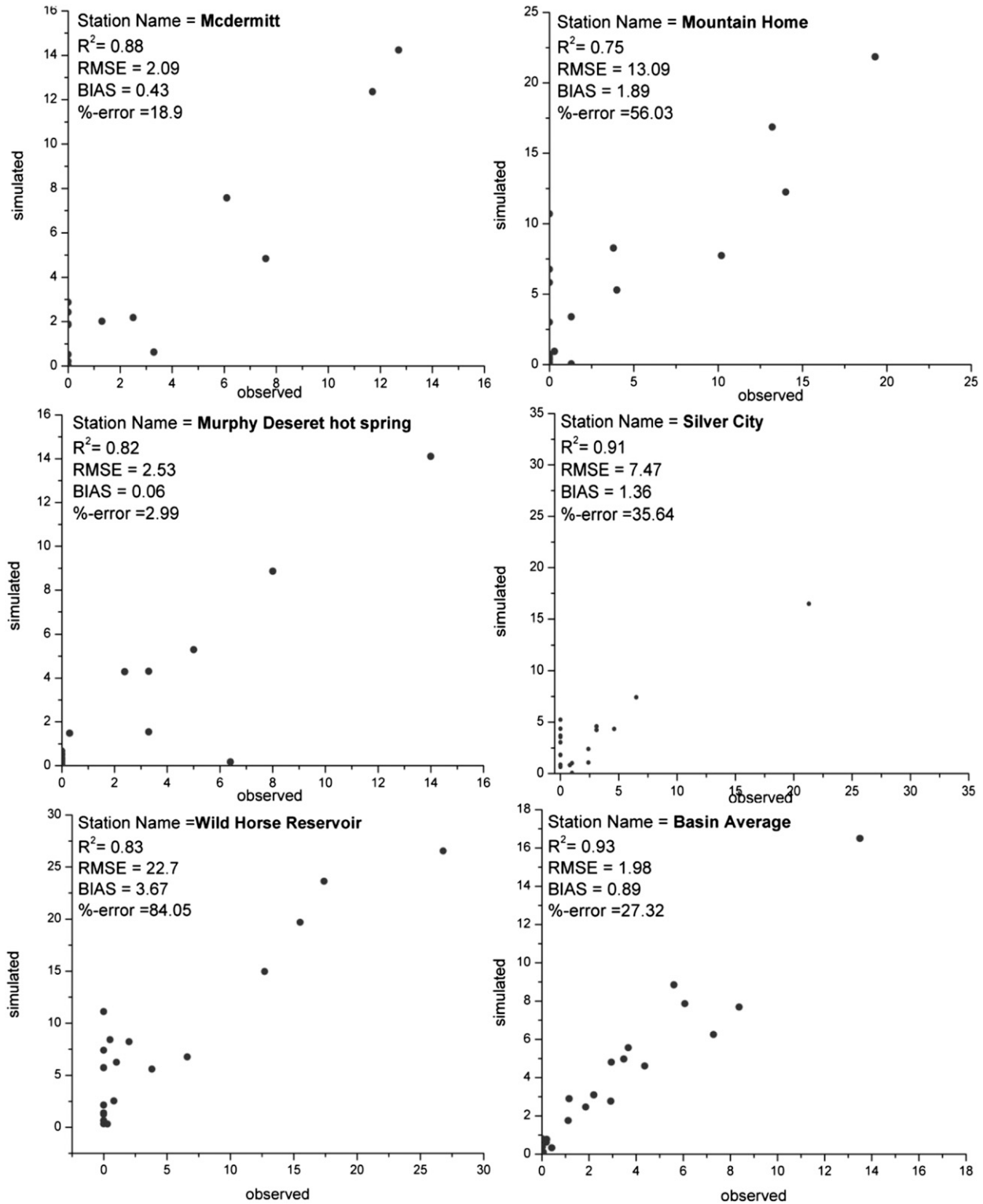
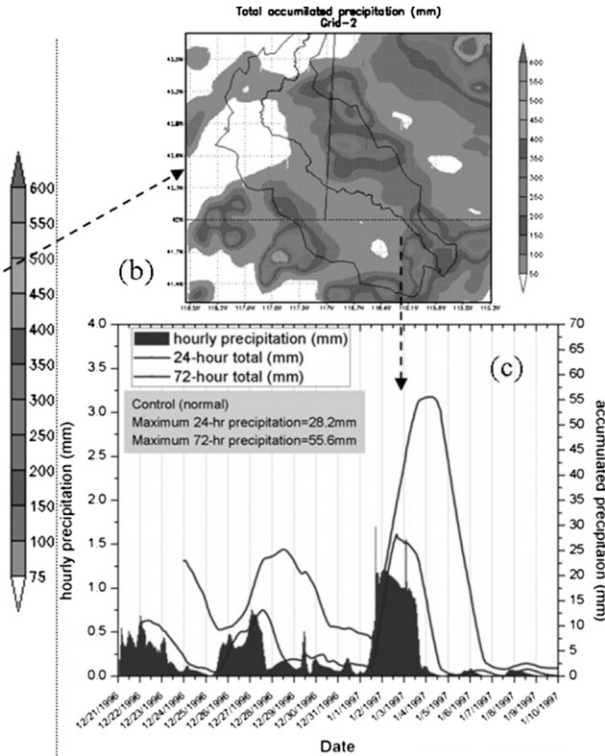
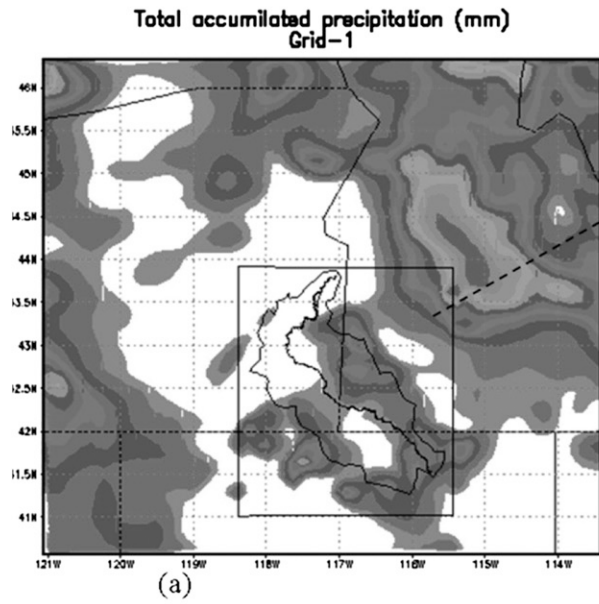


FIG. 5. Scatterplots of ground observation vs RAMS simulated precipitation values with different statistical measures imbedded in each figure for the stations presented in Fig. 4.

AU25

Normal Case of Simulation



Moisture Maximized Case of Simulation

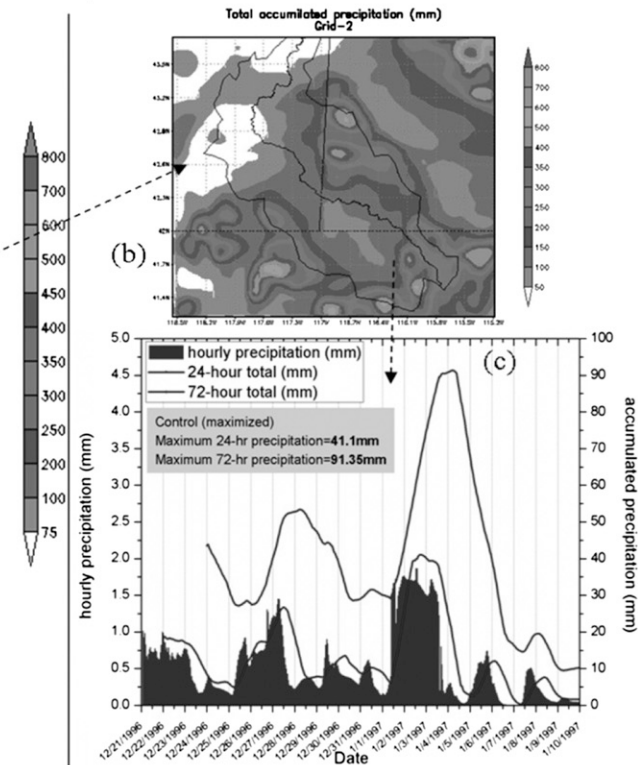
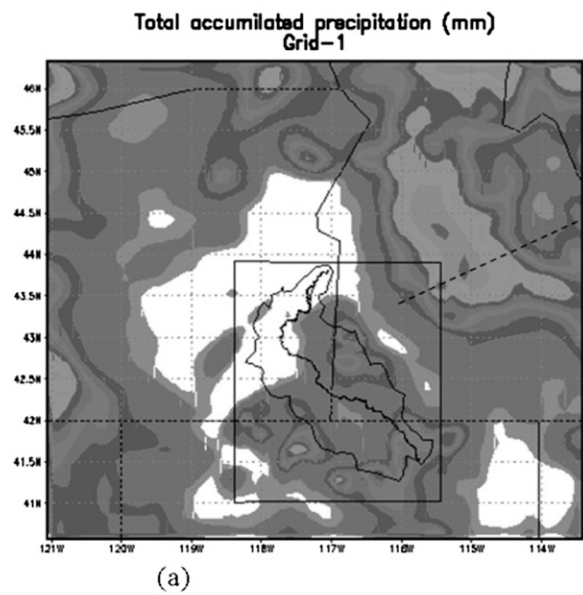
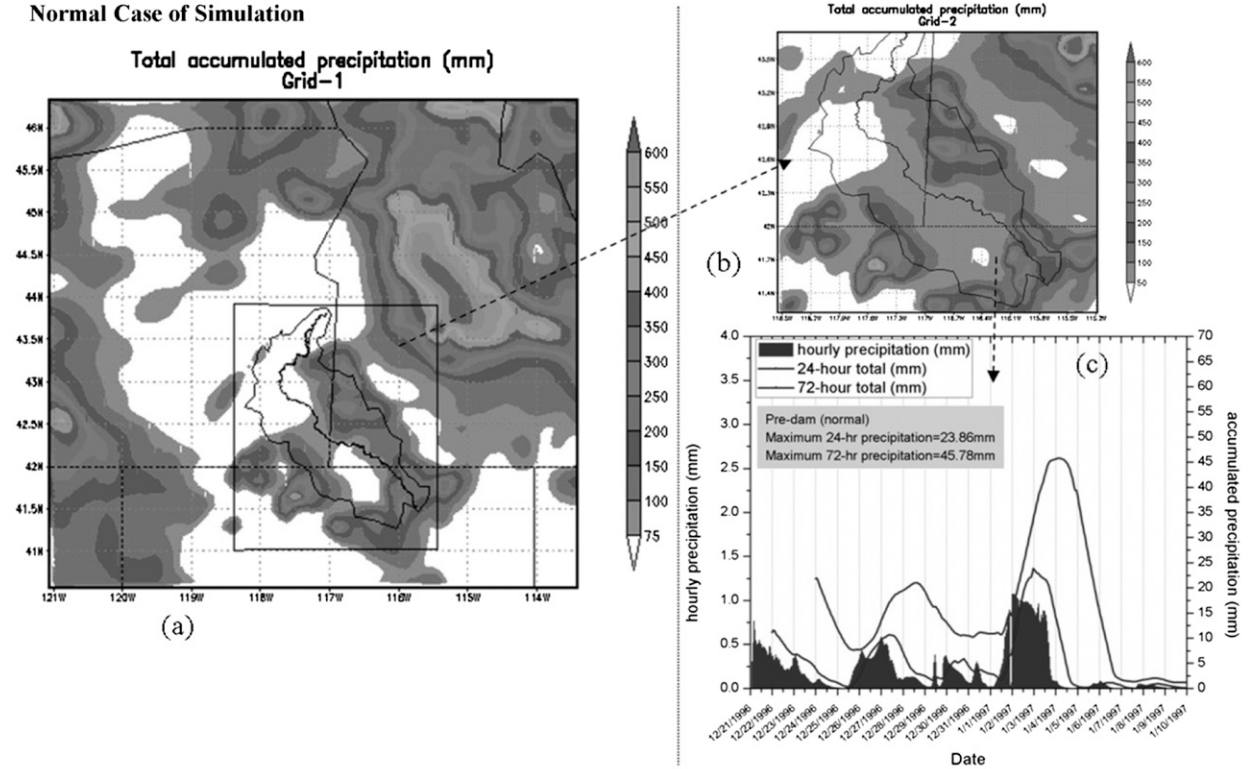


FIG. 6. Total accumulated precipitation (mm) for the control case on (a) grid 1 and (b) grid 2, and (c) the 24- and 72-h moving sums over ORW for (top) normal case and (bottom) moisture-maximized case. Simulation period spans from 21 Dec 1996 to 10 Jan 1997.

Normal Case of Simulation



Moisture Maximized Case of Simulation

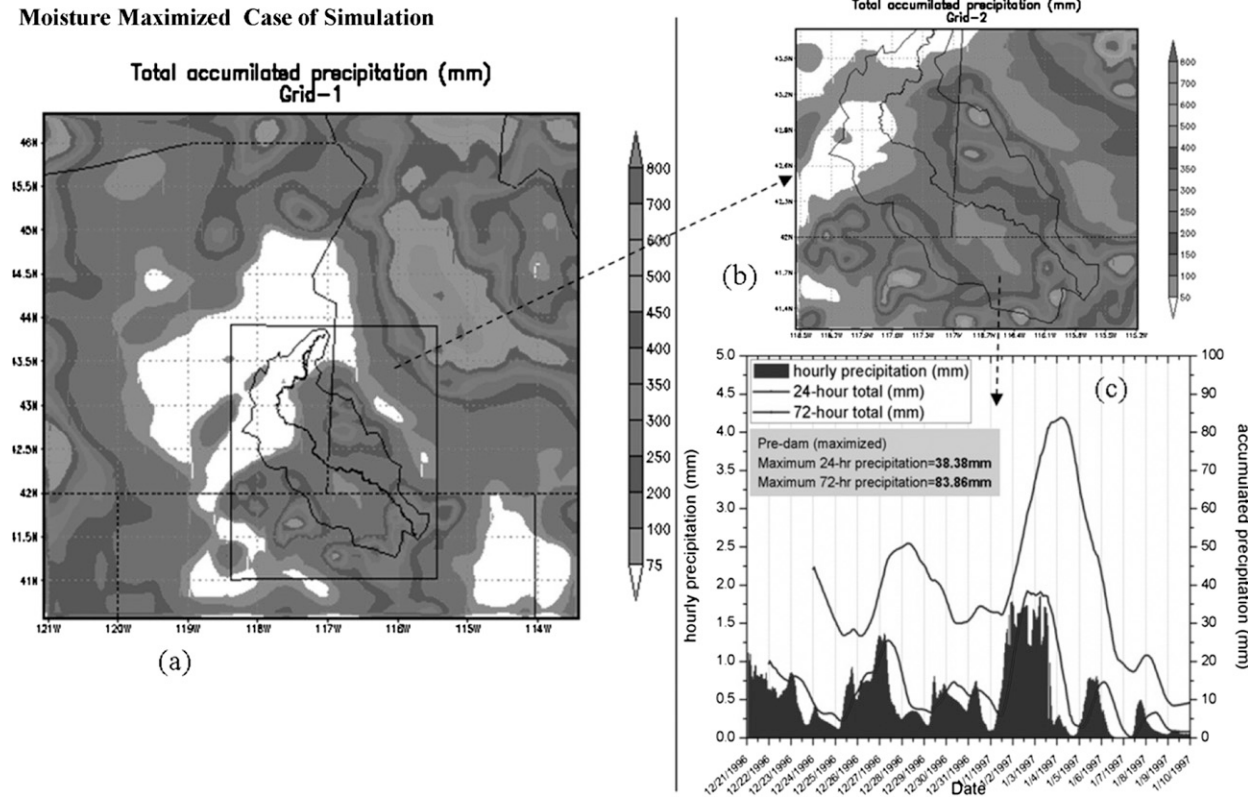


FIG. 7. As in Fig. 6, but for the predam case.

TABLE 5. Summary of 72-h maximum for the four cases (normal case).

Run type	Maximum 72-h precipitation (mm)	Difference from control (mm)	Percent increase/decrease from control (%)
Control	55.6	—	—
Reservoir double	59.3	-3.7	+6.65
Nonirrigation	48.78	6.82	-12.27
Predam	45.78	9.82	-17.66

TABLE 7. Summary of 72-h maximum for the four cases (moisture-maximized case).

Run Type	Maximum 72-h precipitation (mm)	Difference from control (mm)	Percent increase/decrease from control (%)
Control	91.35	—	—
Reservoir double	95.17	-3.82	+4.18
Nonirrigation	85.87	5.48	-6
Predam	83.86	7.49	-8.2

be noted that the 24- and 72-h period moving sums provided in Fig. 6 are labeled by their ending time. For instance, maximum 24-h precipitation was found at 1600 UTC 2 January 1997, and the corresponding 24-h period was therefore from 1600 UTC 1 January to 1600 UTC 2 January 1997. Similarly, the maximum 72-h precipitation was found at 0400 UTC 4 January 1997, and the corresponding 72-h period was therefore from 0400 UTC 1 January to 0400 UTC 4 January 1997. The maximum 24- and 72-h precipitation totals over the ORW were found to be 28.2 and 55.6 mm, respectively. After the moisture maximization was adopted, these values increased to 41.1 mm for 24 h and 91.35 mm for 72 h. The moisture-maximized values represent EPs that resemble the PMP estimated by the standard methods. In general, through the moisture maximization experience, by making the atmosphere moisture nonlimiting, there was a 64% increase in simulated precipitation. Further analysis of the various LULC feedback scenarios with respect to the control are presented in sections 4b(1)–4b(3).

1) THE PREDAM/POSTDAM SCENARIO

The predam represents undisturbed LULC conditions by human interference, which becomes apparent after the dam is constructed (postdam). Hence, in order to understand the effects of the anthropogenic changes introduced in the postdam era, it is essential to investigate the hydrometeorological conditions before

(predam) and after (postdam) the dam construction. According to HYDE classification, the 1930 land use was predominantly grasslands, croplands, and mixed forests downstream of the Owyhee Dam, along with a small urbanized zone (Fig. 2c). This condition is completely transformed after the 1930s, when the dam became operational. Irrigation intensified and the urbanized areas also expanded around the vicinity of the dam (Fig. 2a). Figure 7 shows the accumulated precipitation amount for the predam case (on grids 1 and 2) as well as the 24- and 72-h moving sums for normal and moisture-maximized cases of simulation. The maximum 24- and 72-h totals for the predam were found to be 23.86 and 45.78 mm, respectively. This shows a decrease in simulated values of 4.34 (15.39%) and 9.82 mm (17.66%) in both the 24- and 72-h simulations from the control, respectively. The 24- and 72-h EP after moisture maximization was found to be 38.38 and 83.86 mm, respectively. There was a decrease, from the control, of 2.72 mm (6.62%) in the 24-h total and 7.49 mm (8.2%) in the 72-h total observed. The results are also summarized in Tables 5 and 6 for the normal and Tables 7 and 8 for moisture-maximized cases.

In both the normal and moisture maximized cases, the decrease in the precipitation (during predam scenario) amount compared well with the work of Yusuf and Salami (2009). They evaluated the effect of the Jebba Dam on various hydrometeorological variables, including rainfall within the Niger River basin. Their results

TABLE 6. Summary of 24-h maximum for the four cases (normal case).

Run type	Maximum 24-h precipitation (mm)	Difference from control (mm)	Percent increase/decrease from control (%)
Control	28.18	—	—
Reservoir double	29.32	-1.14	+4.05
Nonirrigation	24.76	3.42	-12.14
Predam	23.86	4.34	-15.39

TABLE 8. Summary of 24-h maximum for the four cases (moisture-maximized case).

Run type	Maximum 24-h precipitation (mm)	Difference from control (mm)	Percent increase/decrease from control (%)
Control	41.1	—	—
Reservoir double	43.97	-2.87	+6.98
Nonirrigation	39.97	1.13	-2.75
Predam	38.38	2.72	-6.62

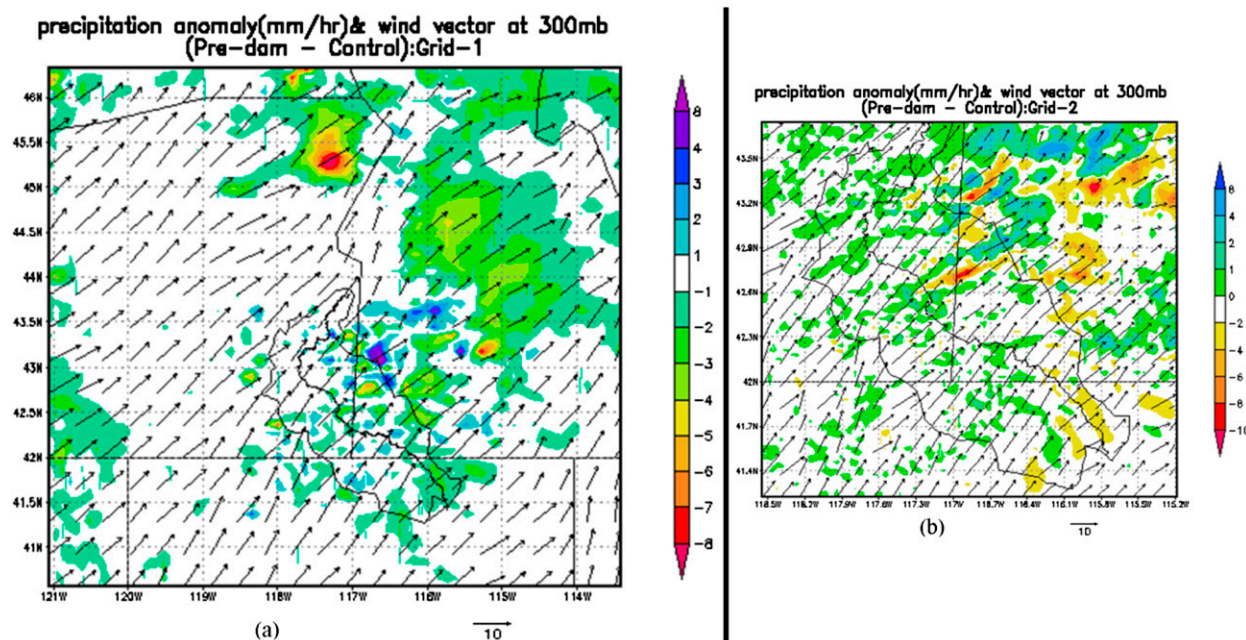


FIG. 8. Precipitation anomaly (mm h^{-1}) of the predam from the control along with the wind vectors at 300-mb level ($1 \text{ mb} = 1 \text{ hPa}$) on (a) grid 1 and (b) grid 2. Figures represent the normal case of simulation.

indicated an increase in precipitation after the construction of the dam. This result is also logical because there was no moisture feedback from the reservoir and only very limited land was used for irrigation during the predam era. Fig. 8 shows the precipitation anomaly of the predam from the control. Areas where the values are negative indicate that the predam produced less precipitation during the simulation period than the control case. It is also important to note that the wind direction is predominantly northeast and that much of the difference is observed in this direction, commonly the downwind region of the dam.

2) RESERVOIR-ATMOSPHERE FEEDBACK SCENARIO

In the postdam era, the presence of the reservoir affected the precipitation pattern. However, in order to isolate the impact of the reservoir from the other effects, one test is to change its size keeping all other LULC conditions the same. From an engineering perspective, it is possible to generate a scenario where the reservoir size is doubled, which is feasible from a terrain analysis. This may not hold true if economic viability is also considered. However, the objective here was to evaluate the sensitivity of precipitation to the surface area of the reservoir. Figure 9 shows the accumulated precipitation amount for the reservoir double case (on grids 1 and 2) as well as the 24- and 72-h moving sums for normal and moisture-maximized cases of simulation. The maximum

24- and 72-h totals for the reservoir double were found to be 29.32 and 59.3 mm, respectively. This shows an increase in simulated values of 1.14 (4.05%) and 3.82 mm (4.18%) in both the 24- and 72-h simulations from the control, respectively (Tables 5, 6). The 24- and 72-h EP after moisture maximization was found to be 43.97 and 95.17 mm, respectively. There was an increase, from the control, of 2.87 mm (6.98%) in the 24-h total and 3.82 mm (4.18%) in the 72-h total observed (Tables 7, 8). The precipitation anomaly of the reservoir double from the control is shown in Fig. 10, where the majority of the regions (on grids 1 and 2) experienced increased precipitation.

The contribution of evaporation within a region to precipitation in that same region (also known as precipitation recycling) was studied in the works of Eltahir and Bras (1996). They estimated that 25% of all rain that fell in the Amazon basin originated from evaporation within the basin. Although a distinction should be made about the extent of the open water evaporation from the transpiration and bare soil evaporation contributions, the results in this study are also indicative of the fact that there perhaps can be precipitation modification through direct evaporation from reservoirs.

3) LAND-ATMOSPHERE FEEDBACK SCENARIO

The land feedback to the atmosphere is evaluated in the form of conversion of the predam land use to irrigation. Presently, much of the downstream area of the

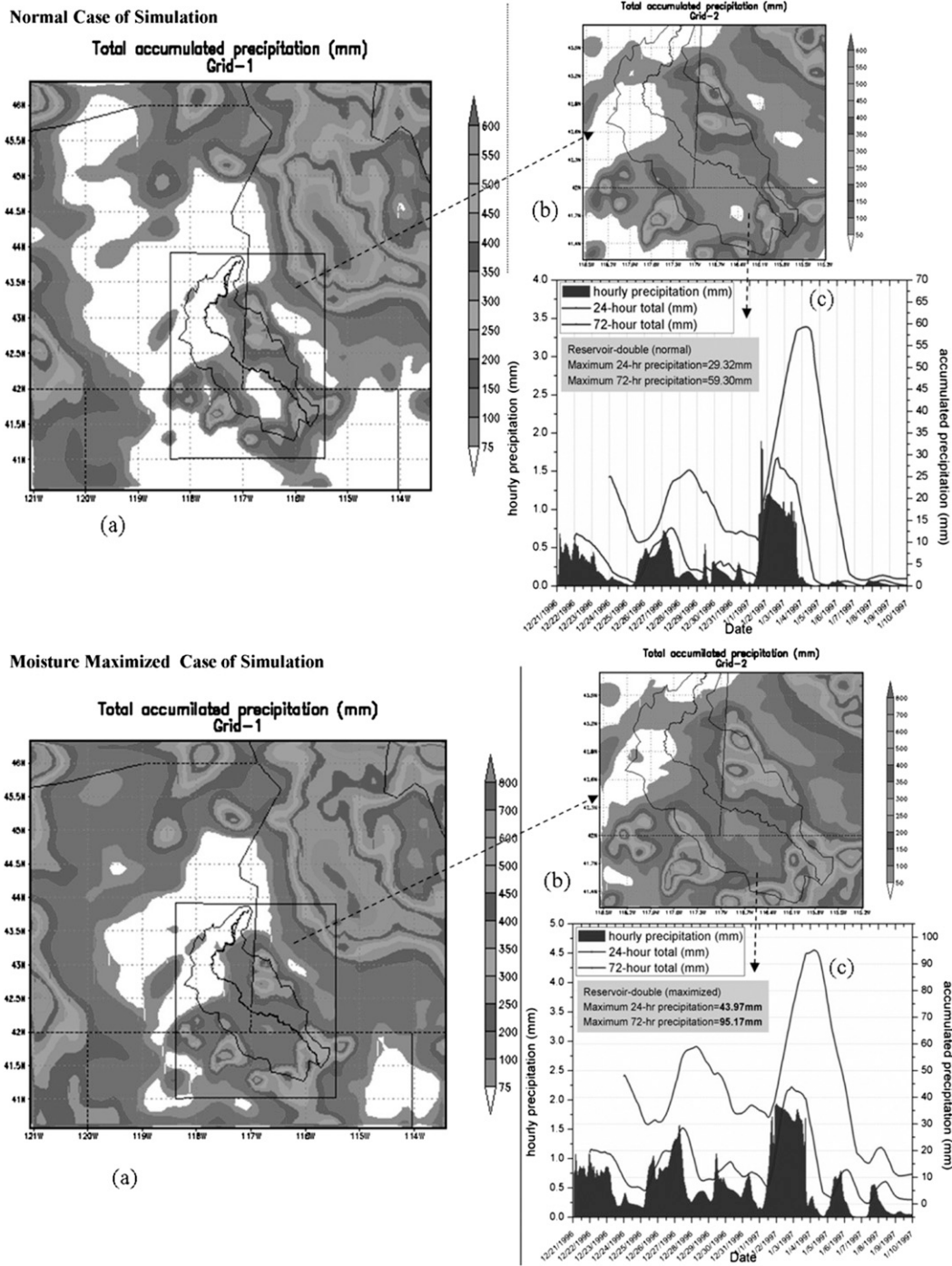


FIG. 9. As in Fig. 6, but for the reservoir double case.

ORW is irrigated extensively. For irrigation contribution analysis, the reverse process of replacing the already existing irrigated region by the nearby predominant land cover type (in this case, grasslands) was performed. This scenario constitutes the nonirrigation case (Fig. 2d). The accumulated precipitation amount for the non-irrigation case (on grids 1 and 2), as well as the 24- and

72-h moving sums for normal and moisture-maximized cases of simulation, are shown in Fig. 11. The maximum 24- and 72-h totals for the nonirrigation were found to be 24.76 and 48.78 mm, respectively. This is a decrease in simulated values of 3.42 (12.14%) and 6.82 mm (12.27%) in both the 24- and 72-h simulations from the control (Tables 5, 6).

E11

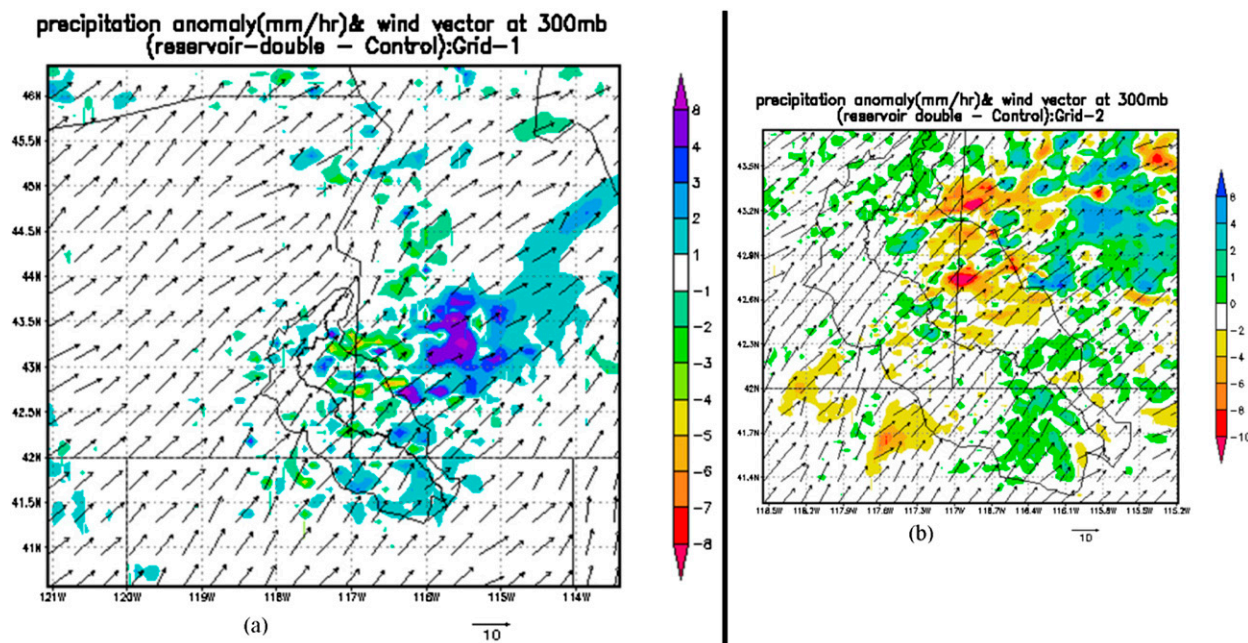


FIG. 10. As in Fig. 8, but for the reservoir double from the control.

The 24- and 72-h EP after moisture maximization was found to be 39.97 and 85.87 mm, respectively. There was a decrease, from the control, of 1.13 mm (2.57%) in the 24-h total and 5.48 mm (6%) in the 72-h total observed (Tables 7, 8). Figure 12 shows the precipitation anomaly of the nonirrigation scenario from the control. Much of the decrease is observed on the downwind (on grid 1) that aligns with the wind direction. Looking at grid 2 (Fig. 12b), it is clear that there are both decreases (within the basin) and increases (downwind). Evidently, because of moist enthalpy changes, precipitation modification caused by irrigation is seen to occur mostly downwind of irrigated lands (DeAngelis 2010), which is also obvious from grid 1 (Fig. 12a) of our analysis.

c. Sensitivity of climate zones and topography on EP modification

In a previous study by Woldemichael et al. (2012), a climatologically and topographically contrasting region (i.e., the ARW and Folsom Dam) was considered in the study of dam/reservoir triggered effects on extreme precipitation modification. In the ARW study, the Folsom Dam predominantly belongs to a climate [interior Mediterranean (Csa) and coastal Mediterranean (Csb) from Köppen classification] that receives rain primarily during the winter season (Figure 13). According to the Köppen climate classification (www.eoearth.org/view/article/162263), such climate is influenced by subtropical highs in fall, summer, and spring and midlatitude cyclones in the winter. On the other hand, the ORW

belongs predominantly to dry (arid) climate [dry semiarid midlatitudes (BSk) and dry arid midlatitudes (BWk)] that receives little precipitation during most of the year. This region usually has a very low relative humidity and an irregular and unreliable rainfall pattern.

In the previous study of the Folsom Dam on ARW, terrain plays a strong role in intensifying the precipitation amount generated on the windward side of the Sierra Nevada. In the Owyhee Dam study, the windward side that is found west of the Cascade Mountains receives much higher precipitation (not shown here) than the leeward side, where the Owyhee Dam/Reservoir resides. Apart from the topographic consideration, which is flat for Owyhee, the considered study period (1996/97) was highly influenced by the presence of ARs, and both of these locations were strongly affected by the same AR event. However, the amount of precipitation generated at the two dam locations shows a significant difference in the 6-day totals (29 December 1996–3 January 1997) (Fig. 14). These 6 days were chosen because it was during this time the AR-assisted moisture resulted in a maximum accumulation of precipitation. In the ARW domain, precipitation totals reached up to 700 mm in 6 days, whereas for the ORW domain, this amount was only 350 mm.

More specifically, the considered LULC change scenarios for each location generated a significant difference, as summarized in Table 9. For the moisture-maximized case, the 72-h EP amount is seen to be affected more by the LULC changes introduced in the

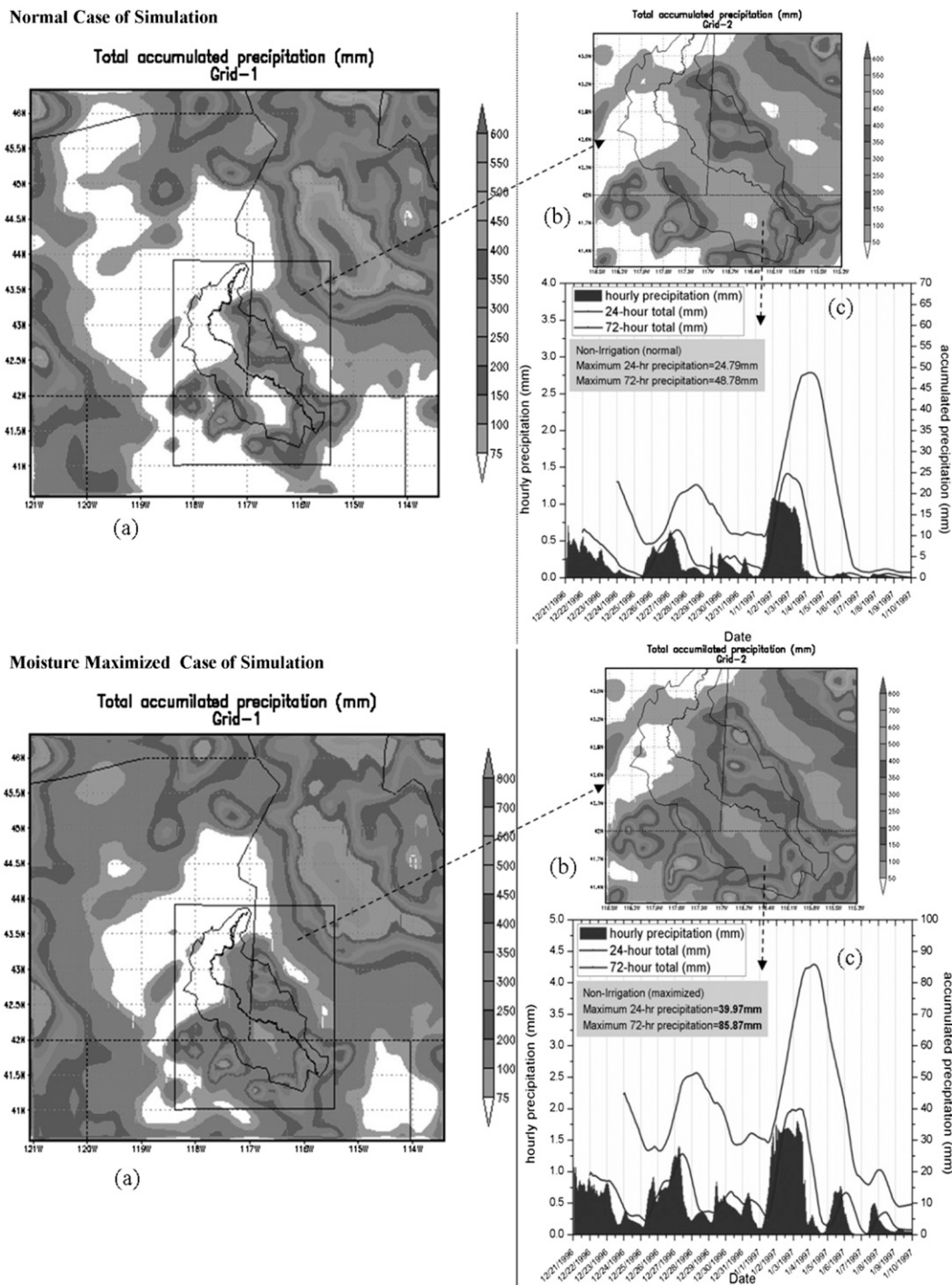


FIG. 11. As in Fig. 6, but for the nonirrigation case.

ORW than the ARW. Similar effects are observed in the normal cases of simulation as well (not shown here). Hence, it is possible to deduce that the effects of post-dam LULC changes on EP are more prominent in arid (semiarid) regions found on a leeward side of mountains

such as the ORW than the ARW, which is characterized by a semiarid climate located on the windward side of mountains. Our finding is consistent with the observational study by Yigzaw et al. (2013, manuscript submitted to *Geophys. Res. Lett.*) that has explored the

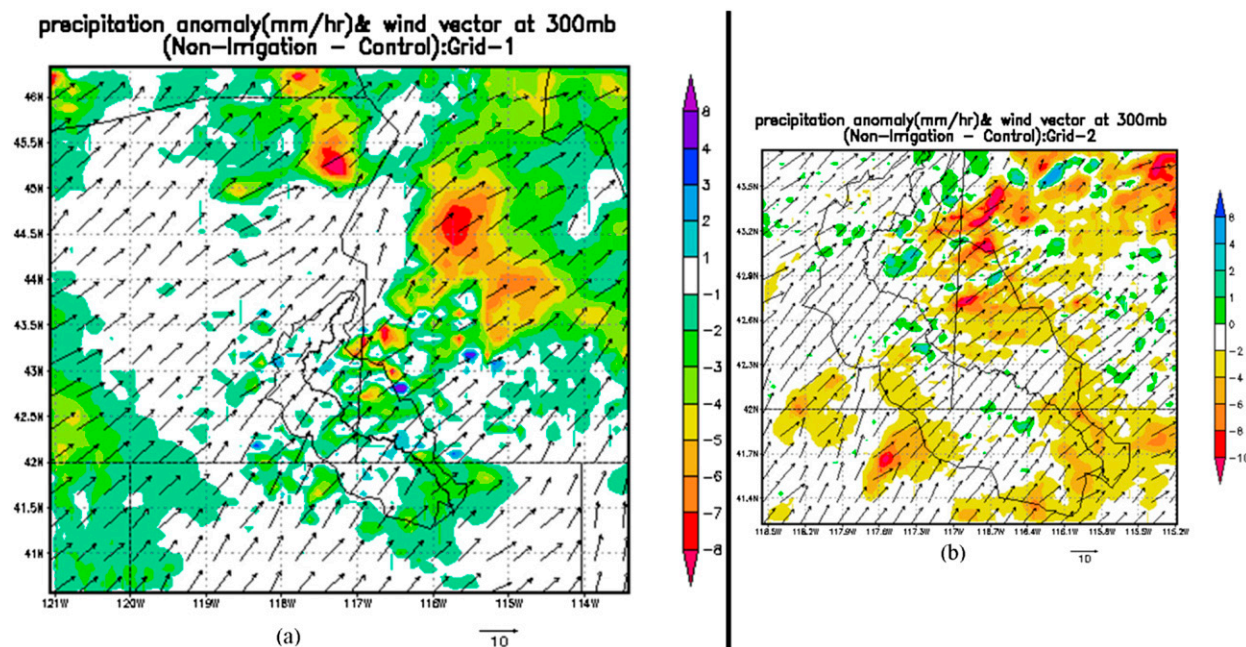


FIG. 12. As in Fig. 8, but for the nonirrigation from the control.

precipitation influence of leeward and windward located dams for the Sierra Nevada and Cascade mountain ranges. Evaluation of the physical processes that are responsible for the variability of the changes introduced in different climate and terrain features is provided by A. T. Woldemichael et al. (2013, unpublished manuscript).

5. Conclusion

This study investigated the integrated effects of the presence of dams/reservoirs and the resulting anthropogenic LULC changes around them on the modification of extreme precipitation. This was accomplished through the use of numerical atmospheric modeling that enabled the incorporation of the various LULC change scenarios in the precipitation simulation. Accordingly, two essential sets of goals were explored. The first goal was analysis of the physical modification of precipitation through dam-triggered anthropogenic changes in LULC. This goal also aims at prioritizing, among the commonly observed LULC changes due to dams, which one of them results in the most prominent alteration of extreme precipitation. It was found out that the LULC changes introduced because of the presence of a dam did in fact modify the magnitude and spatial distribution of extreme precipitation. The predam scenario seemed to have the most significant change in the 24- and 72-h EP amount followed by the nonirrigation scenario (i.e., the impact of irrigation during postdam era). These changes

could further be reinforced by a study of the runoff response through a use of distributed rainfall-runoff models that utilize the estimated EP from this study as a proxy for PMP of standard probable maximum flood (PMF) estimation procedures. Such rainfall-runoff work has already been carried out for the Folsom Dam on the ARW (Yigzaw et al. 2012, 2013).

For the second goal, we tested the premise that no two regions that have a different hydroclimatology and terrain features generate similar hydrometeorological variability for the various postdam LULC scenarios. The ARW is located in a region where abundant rainfall can be received, especially in the winter season. On the other hand, the ORW is located in a region that receives very little rainfall throughout the year because of the predam physical conditions (leeward of the Cascades). By exploring the orographic features (or the lack of thereof), it can be deduced that the precipitation total, either the 24- or 72-h total, simulated in the ARW is much higher than what is expected in ORW. However, the results of the two separate studies indicated that EP on ORW and Owyhee Dam due to postdam LULC changes is much more sensitive to hydroclimatology and terrain features than the ARW and Folsom Dam. This result represents a finding that can be generalized as follows: extreme precipitation in dry arid or semiarid regions in the lee of mountain ranges are more sensitive to the postdam climate feedbacks driven by LULC changes than for such regions that are located on the windward side.

AU12

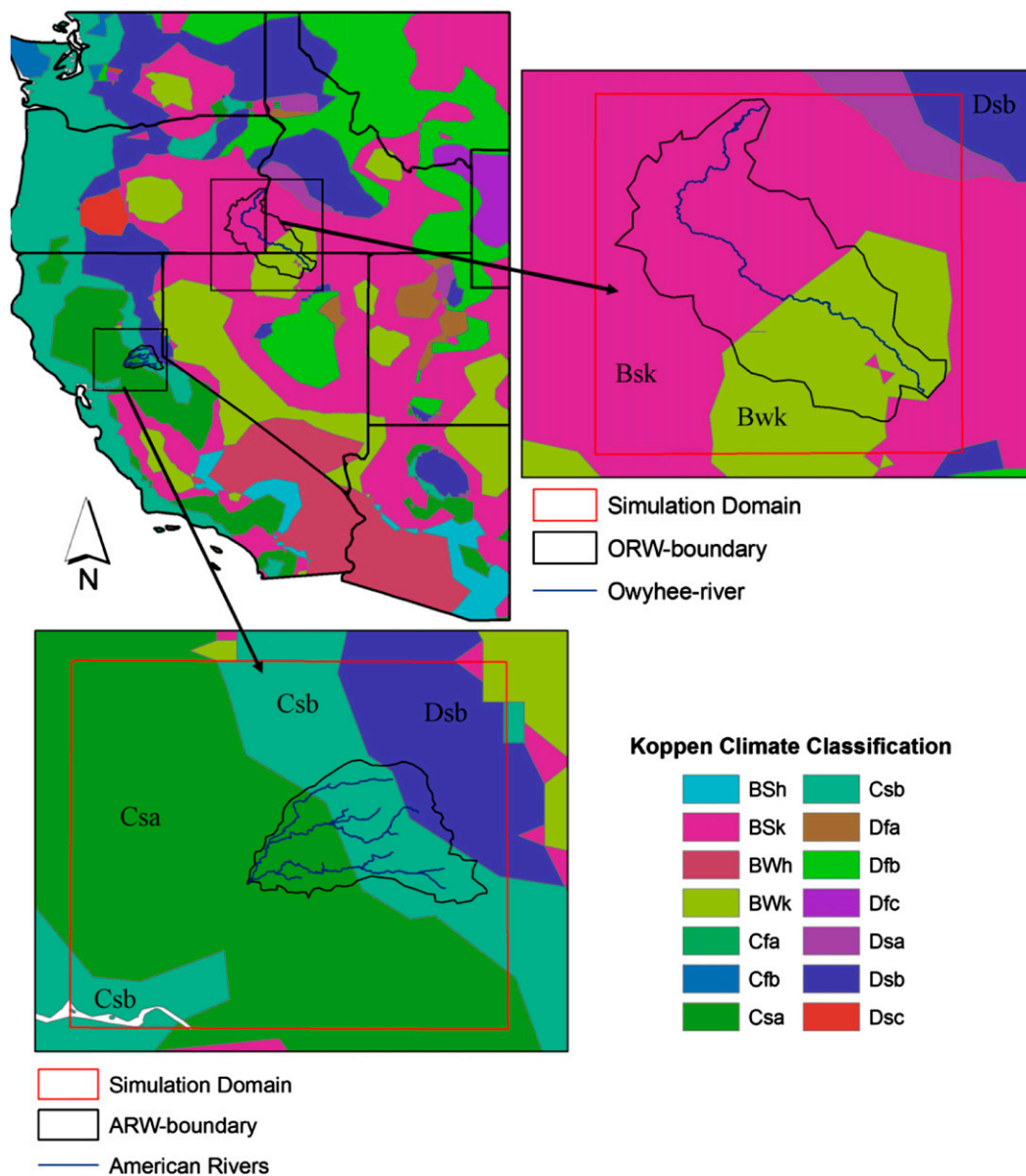


FIG. 13. Köppen climate classifications for the ARW and ORW regions. See text for classification definitions.

Although the focus of the study is not on absolute changes in precipitation values as simulated by the model, a concern that may be raised is the level of confidence one can place in these relative (percent) numbers on change. An earlier study by Woldemichael et al. (2012) explored the level of confidence in the RAMS model results for the setup over the ARW and reported a model simulation noise an order smaller (~0.5%) than the signal (~5%) that was obtained from running the model. Another difficulty in understanding implications that may arise is the plausible mechanism that should be responsible for impact of a small change

in reservoir size into a significant change in extreme precipitation. A change in the size of a reservoir can contribute to modification of precipitation in more indirect (nonlinear) ways than just being a direct source of moisture. For instance, a change in reservoir size can 1) alter that surface and dewpoint temperature; 2) contribute to the partitioning of latent and sensible heat fluxes that in turn result in an increase (decrease) of the amount of water vapor in the atmosphere; and 3) produce variation in low-level wind flow that can affect localized circulations, moisture advection, and convergences. The reader is referred to Pielke and Avissar

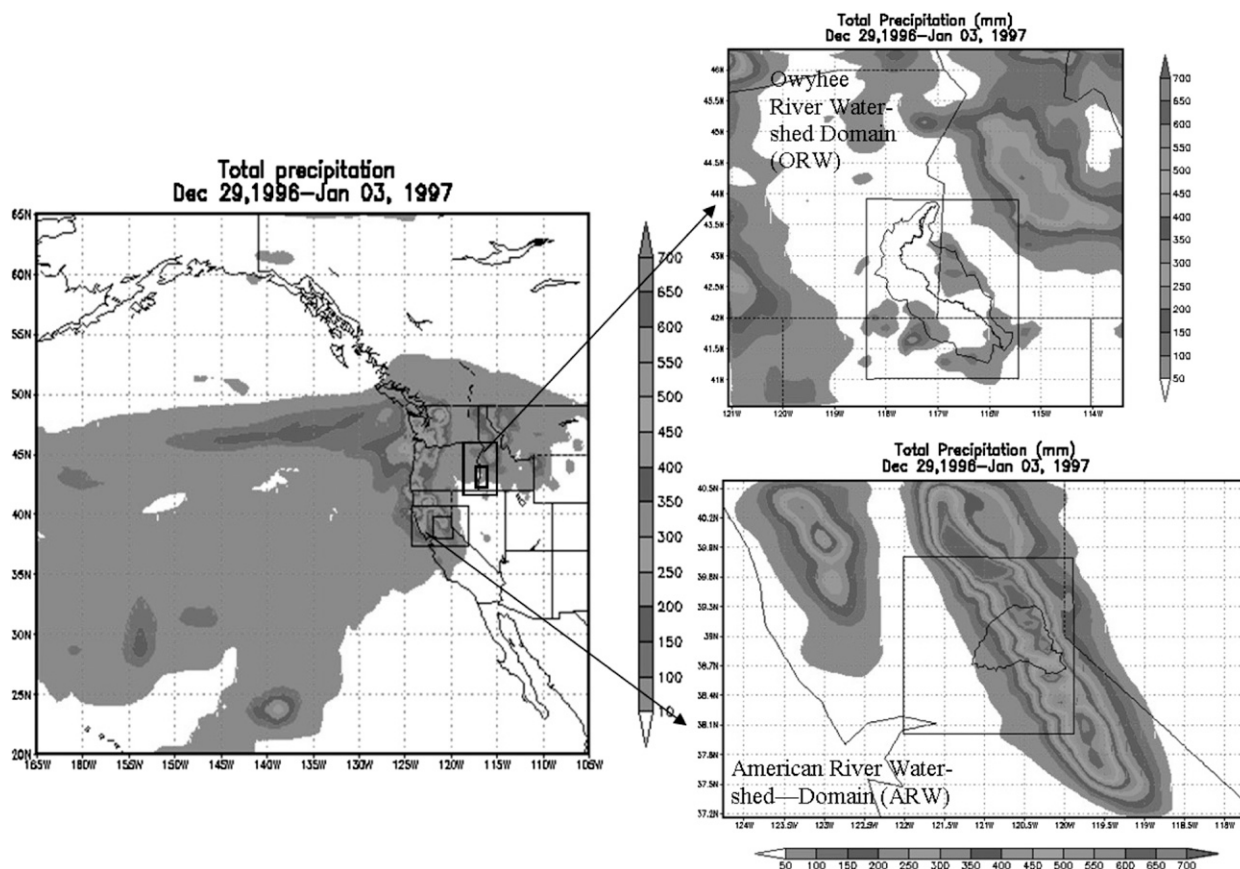


FIG. 14. (left) The 6-day totals of precipitation and on the (top right) ORW domain and (bottom right) ARW domain.

(1990) for a more in-depth explanation of how areal changes in land surface type can impact precipitation patterns.

AU13 A report by Sundaram (2011) claimed that significant progress had been made to integrate the World Commission on Dams' equity, efficiency, sustainability, and accountability in the development of dams in order to meet the current and future water needs. However, the report also indicated that there was plenty of room for significant improvement to address the challenges of sustainability and climate. For the climate domain, our findings suggest that postdam feedbacks resulting from

LULC variability need to be addressed extensively as an additional and essential scenario for dam design and operation for the twenty-first century.

Acknowledgments. The first author (Woldemichael) was supported by the NASA Earth System Science Fellowship Grant NNX12AN34H. The second author (Hossain) acknowledges the support received from NASA SERVIR Grant NNX12AM85G. Third author (Pielke) received support from NSF Grant 1549616.

REFERENCES

Abbs, D. J., 1999: A numerical modeling study to investigate the assumptions used in the calculation of probable maximum precipitation. *Water Resour. Res.*, **35**, 785–796, doi:10.1029/1998WR900013.

Adegoke, J. O., R. A. Pielke Sr., and A. M. Carleton, 2007: Observational and modeling studies of their impacts of agriculture-related land use change on climate in the central U.S. *Agric. For. Meteorol.*, **142**, 203–215, doi:10.1016/j.agrformet.2006.07.013.

Allin, S. R. F., 2004: An examination of the China's Three Gorges Dam Project based on the framework presented in the report of the world commission on dams. M.S. thesis, Dept. of

TABLE 9. Summary of percent increase/decreases on the 72-h moisture-maximized cases (EP) for the ARW and ORW domains.

Run type	Percent increase/decrease from control (%)	
	ARW domain	ORW domain
Control	—	—
Reservoir double	+1.105	+4.18
Nonirrigation	2.94	6
Predam	2.18	8.2

AU14

- XXXXXXX, Virginia Polytechnic Institute and State University, 52 pp. [Available online at http://scholar.lib.vt.edu/theses/available/etd-12142004-125131/unrestricted/SAllin_010304.pdf.]
- AU15** Boucher, O., G. Myhre, and A. Myhre, 2004: Direct human influence of irrigation on atmospheric water vapor and climate. *Climate Dyn.*, **22**, 597–603, doi:10.1007/s00382-004-0402-4.
- Carlson, T. N., and G. A. Sanchez-Azofeifa, 1999: Satellite remote sensing of land use changes in and around San Jose, Costa Rica. *Remote Sens. Environ.*, **70**, 247–256, doi:10.1016/S0034-4257(99)00018-8.
- Chen, L. C., and A. A. Bradley, 2006: Adequacy of using surface humidity to estimate atmospheric moisture availability for probable maximum precipitation. *Water Resour. Res.*, **42**, W09410, doi:10.1029/2005WR004469.
- Cotton, W. R., R. L. McAnelly, and T. Ashby, 2003: Development of new methodologies for determining extreme rainfall. Final Rep. for Contract ENC #C154213, State of Colorado Dept. of Natural Resources, 140 pp. [Available online at <http://rams.atmos.colostate.edu/precip-proj/overnow/index.html>.]
- Daly, C., R. P. Neilson, and D. L. Phillips, 1994: A statistical-topographic model for mapping climatological precipitation over mountainous terrain. *J. Appl. Meteor.*, **33**, 140–158, doi:10.1175/1520-0450(1994)033<0140:ASTMFM>2.0.CO;2.
- DeAngelis, A., F. Dominguez, Y. Fan, A. Robock, M. D. Kustu, and D. Robinson, 2010: Evidence of enhanced precipitation due to irrigation over the Great Plains of the United States. *J. Geophys. Res.*, **115**, D15115, doi:10.1029/2010JD013892.
- Degu, A. M., and F. Hossain, 2012: Investigating the mesoscale impact of artificial reservoirs on frequency of rain during growing season. *Water Resour. Res.*, **48**, W05510, doi:10.1029/2011WR010966.
- Dettinger, M. D., K. Redmond, and D. Cayan, 2004: Winter orographic precipitation ratios in the Sierra Nevada—Large scale atmospheric circulation and hydrologic consequences. *J. Hydrometeorol.*, **5**, 1102–1116, doi:10.1175/JHM-390.1.
- AU16** —, and Coauthors, 2012: Design of quantification of an extreme winter storm scenarios for emergency preparedness and planning exercise in California. *Nat. Hazards*, **60**, 1085–1111, doi:10.1007/s11069-011-9894-5.
- Douglas, E. M., D. Niyogi, S. Frolking, J. B. Yeluripati, R. A. Pielke Sr., N. Niyogi, C. J. Vörösmarty, and U. C. Mohanty, 2006: Changes in moisture and energy fluxes due to agricultural land use and irrigation in the Indian Monsoon Belt. *Geophys. Res. Lett.*, **33**, L14403, doi:10.1029/2006GL026550.
- Eltahir, E. A. B., 1989: A feedback mechanism in annual rainfall. Central Sudan. *J. Hydrol.*, **110**, 323–334, doi:10.1016/0022-1694(89)90195-9.
- , and R. L. Bras, 1996: Precipitation recycling. *Rev. Geophys.*, **34**, 367–378, doi:10.1029/96RG01927.
- Eungul, L., W. J. Sacks, T. N. Chase, and J. A. Foley, 2011: Simulated impacts of irrigation on the atmospheric circulation over Asia. *J. Geophys. Res.*, **116**, D08114, doi:10.1029/2010JD014740.
- FEMA, 2013: Living with dams: Know your risks. Rep. FEMA P-956, 25 pp. [Available at http://www.fema.gov/media-library-data/20130726-1845-25045-7939/fema_p_956_living_with_dams.pdf.]
- Gangoiti, G., and Coauthors, 2011a: Origin of the water vapor responsible for the European extreme rainfalls of August 2002: 1. High-resolution simulations and tracking of air masses. *J. Geophys. Res.*, **116**, D21102, doi:10.1029/2010JD015530.
- , and Coauthors, 2011b: Origin of the water vapor responsible for the European extreme rainfalls of August 2002: 2. A new methodology to evaluate evaporative moisture sources, applied to the August 11–13 central European rainfall episode. *J. Geophys. Res.*, **116**, D21103, doi:10.1029/2010JD015538.
- Gero, A., A. J. Pitman, G. T. Narisma, C. Jacobson, and R. A. Pielke Sr., 2006: The impact of land cover change on storms in the Sydney Basin, Australia. *Global Planet. Change*, **54**, 57–78, doi:10.1016/j.gloplacha.2006.05.003.
- Graf, W. L., 1999: Dam nation: A geographic census of American dams and their large-scale hydrologic impacts. *Water Resour. Res.*, **35**, 1305–1311, doi:10.1029/1999WR900016.
- Hammond, M., 2013: The Grand Ethiopian Renaissance Dam and the Blue Nile implications for transboundary water governance. GWF Discussion Paper 1307, Global Water Forum, Canberra, Australia, 5 pp. [Available online at <http://www.globwaterforum.org/wp-content/uploads/2013/02/The-Grand-Ethiopian-Renaissance-Dam-and-the-Blue-Nile-Implications-for-transboundary-water-governance-GWF-1307.pdf>.]
- Hansen, E. M., 1987: Probable maximum precipitation for design floods in the United States. *J. Hydrol.*, **96**, 267–278, doi:10.1016/0022-1694(87)90158-2.
- AU17** —, D. D. Fenn, P. Corrigan, J. L. Vogel, L. C. Schreiner, and R. W. Stodt, 1994: Probable maximum precipitation—Pacific Northwest states. Hydrometeorological Rep. 57, National Weather Service, Silver Spring, MD, 353 pp. [Available online at http://www.nws.noaa.gov/oh/hdsc/PMP_documents/HMR57.pdf.]
- Harrington, J. Y., 1997: The effects of radiative and microphysical processes on simulated warm and transition season Arctic stratus. Ph.D. dissertation, Colorado State University, 289 pp.
- Hossain, F., A. M. Degu, W. Yigzaw, D. Niyogi, S. Burian, J. M. Shepherd, and R. A. Pielke Sr., 2012: Climate feedback-based considerations to dam design, operations and water management in the 21st century. *J. Hydrol. Eng.*, **17**, 837–850, doi:10.1061/(ASCE)HE.1943-5584.0000541.
- Huff, T. E., 1986: Urban hydrometeorology review. *Bull. Amer. Meteor. Soc.*, **67**, 703–711.
- International Commission on Large Dams, 1999: Benefits and concerns about dams. XX pp.
- AU18** Jeton, A. E., M. D. Dettinger, and J. L. Smith, 1996: Potential effects of climate change on stream flow, eastern and western slopes of the Sierra Nevada, California and Nevada. USGS Water-Resources Investigations Rep. 95-4260, 44 pp. [Available online at <http://pubs.usgs.gov/wri/1995/4260/report.pdf>.]
- Jin, M., J. M. Shepherd, and C. Peters-Lidard, 2007: Development of a parameterization for simulating the urban temperature hazard using satellite observations in climate model. *Nat. Hazards*, **43**, 257–271, doi:10.1007/s11069-007-9117-2.
- Kain, J. S., and M. Fritsch, 1993: Convective parameterization for mesoscale models: The Kain-Fritsch scheme. *The Representation of Cumulus Convection in Numerical Models, Meteor. Monogr.*, No. 24, Amer. Meteor. Soc., 165–170.
- Kalnay, E., and Coauthors, 1996: The NCEP/NCAR 40-Year Reanalysis Project. *Bull. Amer. Meteor. Soc.*, **77**, 437–471, doi:10.1175/1520-0477(1996)077<0437:TNYRYP>2.0.CO;2.
- Klein Goldewijk, K., A. Beusen, G. van Drecht, and M. de Vos, 2011: The HYDE 3.1 spatially explicit database of human induced land use change over the past 12,000 years. *Glob. Ecol. Biogeogr.*, **20**, 73–86, doi:10.1111/j.1466-8238.2010.00587.x.
- Klemp, J. B., and R. B. Wilhelmson, 1978: The simulation of three-dimensional convective storm dynamics. *J. Atmos. Sci.*, **35**, 1070–1096, doi:10.1175/1520-0469(1978)035<1070:TSOTDC>2.0.CO;2.
- Kunstmann, H., and H. R. Knoche, 2011: Tracing water pathways from the land surface through the atmosphere: A new RCM-based evapotranspiration tagging method and its application

- to the Lake Volta region in West Africa. *Proc. Third iLEAPS Science Conf.*, Garmisch-Partenkirchen, Germany, Karlsruhe Institute of Technology, 2 pp. [Available online at http://www.ileaps.org/sites/ileaps.org/files/sci_conf_book/pdf/20110415195004_Kunstmann-ET-Tagging-ILEAPS2011-GAP.pdf.]
- Liston, G. E., and R. A. Pielke, 2000: A climate version of the Regional Atmospheric Modeling System. *Theor. Appl. Climatol.*, **66**, 29–47, doi:10.1007/s007040070031.
- Marks, D., T. Link, A. Winstral, and D. Garen, 2001: Simulating snowmelt processes during rain-on-snow over a semi-arid mountain basin. *Ann. Glaciol.*, **32**, 195–202, doi:10.3189/172756401781819751.
- Marshall, C. H., Jr., R. A. Pielke Sr., L. T. Steyaert, and D. A. Willard, 2004: The impact of anthropogenic land-cover change on the Florida peninsula sea breezes and warm season sensible weather. *Mon. Wea. Rev.*, **132**, 28–52, doi:10.1175/1520-0493(2004)132<0028:TIOALC>2.0.CO;2.
- Meyers, M. P., R. L. Walko, J. Y. Harrington, and W. R. Cotton, 1997: New RAMS cloud microphysics parameterization. Part II: The two moment scheme. *Atmos. Res.*, **45**, 3–39, doi:10.1016/S0169-8095(97)00018-5.
- Narisma, T., and A. J. Pitman, 2006: Exploring the sensitivity of the Australian climate to regional land-cover-change scenarios under increasing CO₂ concentrations and warmer temperature. *Earth Interact.*, **10**, doi:10.1175/EI154.1.
- Nicolini, M., A. C. Torres, and P. Salio, 2002: Enhanced precipitation over southeastern South America related to strong low-level jet events during austral warm season. *Meteorologica*, **27**, 59–69. [Available online at <http://www.cenamet.org.ar/27.3.pdf>.]
- Ohara, N., M. L. Kavvas, S. Kure, Z. Q. Chen, S. Jang, and E. Tan, 2011: Physically based estimation of maximum precipitation over American River watershed, California. *J. Hydrol. Eng.*, **16**, 351–361, doi:10.1061/(ASCE)HE.1943-5584.0000324.
- Oxlade, C., 2006: *Dams*. 2nd ed. Heinemann Library, 32 pp.
- Pasqui, M., B. Gozzini, D. Grifoni, F. Meneguzzo, G. Messeri, M. Pieri, M. Rossi, and G. Zipoli, 2000: Performances of the operational RAMS in a Mediterranean region as regards to quantitative precipitation forecasts: Sensitivity of precipitation and wind forecasts to the representation of land cover. *Fourth RAMS Users Workshop*, New Brunswick, NJ, Rutgers University, 22 pp. [Available online at <http://www.atmet.com/html/workshop/presentations/massimiliano.pdf>.]
- Pielke, R. A., Sr., 2001: Influence of the spatial distribution of vegetation and soils on the prediction of cumulus convective rainfall. *Rev. Geophys.*, **39**, 151–177, doi:10.1029/1999RG000072.
- , and R. Avissar, 1990: Influence of landscape structure on local and regional climate. *Landscape Ecol.*, **4**, 133–155, doi:10.1007/BF00132857.
- , and Coauthors, 1992: A comprehensive meteorological modeling system—RAMS. *Meteor. Atmos. Phys.*, **49**, 69–91, doi:10.1007/BF01025401.
- , R. L. Walko, L. T. Steyaert, P. L. Vidale, G. E. Liston, W. A. Lyons, and T. N. Chase, 1999: The influence of anthropogenic landscape changes on weather in south Florida. *Mon. Weather Rev.*, **127**, 1663–1673, doi:10.1175/1520-0493(1999)127<1663:TIOALC>2.0.CO;2.
- Ray, D. K., U. S. Nair, R. M. Welch, Q. Han, J. Zeng, W. Su, T. Kikuchi, and T. J. Lyons, 2003: Effects of land use in Southwest Australia. 1: Observations of cumulus cloudiness and energy fluxes. *J. Geophys. Res.*, **108**, 4414, doi:10.1029/2002JD002654.
- Rial, J., and Coauthors, 2004: Nonlinearities, feedbacks and critical thresholds within the Earth's climate system. *Climatic Change*, **65**, 11–38, doi:10.1023/B:CLIM.0000037493.89489.3f.
- Richter, B. D., and G. A. Thomas, 2007: Restoring environmental flows by modifying dam operations. *Ecol. Soc.*, **12**, 12. [Available online at <http://www.ecologyandsociety.org/vol12/iss1/art12/>.]
- Rosenfeld, A., H. Akbari, and S. E. Bretz, 1995: Mitigation of urban heat islands: Materials, utility programs, updates. *Energy Build.*, **22**, 255–265, doi:10.1016/0378-7788(95)00927-P.
- Sacks, W. J., B. I. Cook, N. Buenning, S. Levis, and J. H. Helkowski, 2008: Effects of global irrigation on the near surface climate. *Climate Dyn.*, **33**, 159–175, doi:10.1007/s00382-008-0445-z.
- Saxena, K. R., 2004: *Dams: Incidents and Accidents*. CRC Press, 240 pp.
- Schleifer, Y., 2008: Turkey revives stalled \$32 billion GAP dam and irrigation project. *The Christian Science Monitor*, 28 May. [Available online at www.csmonitor.com/layout/set/r14/World/Europe/2008/0528/p12s01-woeu.html.]
- Schneider, N., W. Eugster, and B. Schichler, 2004: The impact of historical land-use changes on the near-surface atmospheric conditions on the Swiss Plateau. *Earth Interact.*, **8**, doi:10.1175/1087-3562(2004)008<0001:TIOHLC>2.0.CO;2.
- Segal, M., Z. Pan, R. W. Turner, E. S. Takle, 1998: On the potential impact of irrigated areas in North America on summer rainfall caused by large-scale systems. *J. Appl. Meteor.*, **37**, 325–331, doi:10.1175/1520-0450-37.3.325.
- Shepherd, J. M., 2005: A review of current investigations of urban-induced rainfall and recommendations for the future. *Earth Interact.*, **9**, doi:10.1175/EI156.1.
- Stohlgren, T. J., N. C. Thomas, R. A. Pielke Sr., T. G. F. Kittles, and J. S. Baron, 1998: Evidence that local land use practices influence regional climate, vegetation, and stream flow patterns in adjacent natural areas. *Global Change Biol.*, **4**, 495–504, doi:10.1046/j.1365-2486.1998.t01-1-00182.x.
- Sundaram, M., 2011: Ten years after the World Commission on Dams Report: Where are we? *Proc. 31st Annual USSD Conf.*, San Diego, CA, U.S. Society on Dams, 51–67. [Available online at <http://ussdams.com/proceedings/2011Proc/51-68.pdf>.]
- Tan, E., 2010: Development of a methodology for probable maximum precipitation estimation over the American River Watershed using the WRF model. Ph.D. dissertation, University of California, Davis, 195 pp.
- Tomlinson, E. M., and W. D. Kappel, 2009: Dam safety: Revisiting PMPs. Hydroworld.com. [Available online at <http://www.hydroworld.com/articles/hr/print/volume-28/issue-7/cover-story/dam-safety-revisiting.html>.]
- Tremback, C. J., G. J. Tripoli, and W. R. Cotton, 1985: A regional scale atmospheric numerical model including explicit moist physics and a hydrostatic time-split scheme. Preprints, *7th Conference on Numerical Weather Prediction*, Montreal, QC, Canada, Amer. Meteor. Soc., 433–434.
- Tripoli, G. J., and W. R. Cotton, 1980: A numerical investigation of several factors contributing to the observed variable intensity of deep convection over South Florida. *J. Appl. Meteor.*, **19**, 1037–1063, doi:10.1175/1520-0450(1980)019<1037:ANIOSF>2.0.CO;2.
- , and —, 1982: The Colorado State University three-dimensional cloud/mesoscale model. Part I: General theoretical framework and sensitivity experiments. *J. Rech. Atmos.*, **16**, 185–220.
- Trusilova, K., M. Jung, G. Churkina, U. Karstens, M. Heimann, M. Claussen 2008: Urbanization impacts on the climate in

AU19

AU20

Europe: Numerical experiments by the PSU-NCAR Mesoscale Model (MM5). *J. Appl. Meteor. Climatol.*, **47**, 1442–1455, doi:10.1175/2007JAMC1624.1.

USACE, 2005: Stochastic modeling of extreme floods on the American River at Folsom dam—Flood-frequency curve extension. USACE Rep., 398 pp. [Available online at http://www.mgsengr.com/damsafetyfiles/NRC2013/AmericanRiver_CurveExtension_FinalReport.pdf.]

U.S. Bureau of Reclamation, 2009: The story of Owyhee Project. Informational pamphlet, 3 pp. [Available online at <http://www.usbr.gov/pn/project/bochures/owyheeproject.pdf>.]

Walko, R. L., and C. J. Tremback, 2002: RAMS: Regional Atmospheric Modeling System, version 4.3/4.4: Introduction to RAMS 4.3/4.4. ASTER Div., Mission Res., Inc., Fort Collins, CO, 11 pp. [Available online at <http://www.atmet.com/html/docs/rams/ug44-rams-intro.pdf>.]

AU21

—, and —, 2005: Modification for the transition from LEAF-2 to LEAF-3. ATMET Tech. Note 1, 13 pp. [Available online at <http://www.atmet.com/html/docs/rams/RT1-leaf2-3.pdf>.]

WMO, 1986: Manual for estimation of probable maximum precipitation. 2nd ed. Operational Hydrology Rep. 1, 298 pp.

Woldemichael, A. T., F. Hossain, R. Pielke Sr., and A. Beltrán-Przekurat, 2012: Understanding the impact of dam-triggered land use/land cover change on the modification of extreme precipitation. *Water Resour. Res.*, **48**, W09547, doi:10.1029/2011WR011684.

Yigzaw, W., F. Hossain, and A. Kalyanapu, 2012: Impact of artificial reservoir size and land use/land cover patterns on estimation of probable maximum precipitation and flood: Case of Folsom Dam on American River. *J. Hydrol. Eng.*, **18**, 1180–1190, doi:10.1061/(ASCE)HE.1943-5584.0000722.

—, —, and —, 2013: Comparison of PMP-driven probable maximum floods with flood magnitudes due to increasingly urbanized catchment: The Case of American River watershed. *Earth Interact.*, **17**, doi:10.1175/2012EI000497.1.

—, —, and T. Chronis, 2013: Precipitation modification around large dams in orographic environments: The case of Cascade Range and Sierra Nevada. *Geophys. Res. Lett.*, submitted.

AU22

Yusuf, K. O., and A. W. Salami, 2009: Influence of Jebba Hydro-power Dam on statistical distribution of hydro-meteorological variables in Niger River Basin, Nigeria. *Proc. First Annual Civil Engineering Conf.*, Ilorin, Nigeria, University of Ilorin, 32–40.

